BIOMECHANICAL AND RADIOLOGICAL EVALUATION OF THE BONE-IMPLANT INTERFACE OF NEW BIODEGRADABLE IMPLANTS IN COMPARISON TO CONVENTIONAL TITANIUM PINS

–

FINDINGS IN A TRANSCORTICAL RAT MODEL

Diplomarbeit

Zur Erlangung des akademischen Grades

DOKTOR DER GESAMTEN HEILKUNDE (Dr. med. univ.)

an der

MEDIZINISCHEN UNIVERSITÄT GRAZ

eingereicht von

RICHARD A. LINDTNER

Matrikelnummer: 0120596

Ausgeführt an der

UNIVERSITÄTSKLINIK FÜR KINDERCHIRURGIE, GRAZ

Unter der Anleitung von

PD DR. ANNELIE-MARTINA WEINBERG

Graz, am 30.4.2009

GUTACHTER:

PD DR. ANNELIE-MARTINA WEINBERG

Universitätsklinik für Kinderchirurgie, Graz

UNIV.-PROF. DR. WOLFGANG GRECHENIG

Universitätsklinik für Unfallchirurgie, Graz

EIDESSTATTLICHE ERKLÄRUNG

Ich erkläre ehrenwörtlich, dass ich die vorliegende Arbeit selbständig und ohne fremde Hilfe verfasst habe, andere als die angegebenen Quellen nicht verwendet habe und die den benutzen Quellen wörtlich oder inhaltlich entnommenen Stellen als solche kenntlich gemacht habe.

Graz, am 30.4.2009

Richard A. Lindtner

ACKNOWLEDGEMENT

First, I am grateful to my adviser Priv.-Doz. Dr. Annelie-Martina Weinberg and to Dr. Christoph Castellani who provided me the great chance to work within this research group and introduced me to the field of experimental research.

This extensive project would not have been realised without the contribution of several cooperators:

Thus, I want to thank Professor Elmar Tschegg and Dr. Michael Jamek (Institute of Solid State Physics, Vienna University of Technology) for providing their experience and technical assistance, Bakk. tech. Gerald Holzlechner for designing the test fixture, Gerald Zanoni (Ludwig Boltzmann Institute for Experimental and Clinical Traumatology and Research Center for Traumatology of the AUVA, Vienna) for carrying out microfocus computed tomography scans and Professor Stefanie Tschegg (Department of Material Sciences and Process Engineering University of Natural Resources and Applied Life Sciences, Vienna) for performing scanning electron microscopic examinations.

Furthermore, I am especially grateful to my partner Petra, my best friend Dominik Weihs and my sister Christina who encouraged me when I was dejected and exhausted.

Primarily I want to thank my parents who have always been and still are a tremendous source of love, compassion, support, encouragement and patience.

Dedicated to my parents in love and gratitude.

TABLE OF CONTENTS

ABBREVIATIONS

BIC	Bone-implant contact area
BV/TV	Bone volume per tissue volume
F_{max}	Maximum pushout force
J	Joule
mm	Millimeter
N	Newton
PDO	Poly(dioxanone)
PGA	Poly(glycolide acid)
PLA	Poly(lactide acid)
PLGA	Poly(lactic-co-glycolic acid)
PLLA	Poly(L-lactide acid)
ROI	Region of interest
SR	Self-reinforced
σ_u	Ultimate Shear Strength
Tb.Th.	Trabecular thickness
vs.	versus
VOI	Volume of interest
µCT	Microfocus computed tomography

LIST OF FIGURES

LIST OF TABLES

ABSTRACT

BACKGROUND: In trauma surgery osteosynthesis aims on early mobilisation of the patient with quick reintegration to work, school and family. However, fracture fixation devices made of conventional titanium as well as of bioabsorbable polymers have several drawbacks in clinical practice. The former are associated with stress shielding phenomenons and have to be removed frequently (especially in paediatric trauma surgery), whereas the latter may cause adverse tissue reactions and exhibit limited mechanical properties. Therefore, we evaluated a newly developed implant made of a magnesium alloy (Mg implants) which is supposed to combine excellent strength retention properties of metallic implants with biodegradability of polymers.

METHODS: In this comparative study, three different types of uncoated smooth cylindrical implants were used: novel Mg pins, new poly(lactic-co-glycolic acid) (PLGA) implants and conventional commercially pure titanium pins. All implants were placed transcortically in the middiaphysis of the femoral bone of 108 Sprague-Dawley rats. Pushout testing, microfocus computed tomography, fluorescent labelling, lightmicroscopic and exemplary scanning electron microscopic examination of the tested implants were performed after an implantation period of 1, 3 as well as 6 months to assess osseointegration.

RESULTS: Pushout testing yielded highly significantly greater median maximum push out forces as well as ultimate shear strengths in Mg implants than in titanium and PLGA pins after each implantation period. Moreover, microfocus computed tomography revealed significantly higher mean bone-implant contact area in Mg implants than in titanium implants after 1 and 6 months of implantation and than in PLGA implants after 1 month. In addition, no local or systemic inflammatory reactions were observed in any of the investigated implant types.

CONCLUSION: This study indicates that these novel biodegradable Mg implants are superior to new bioabsorbable PLGA and even to titanium pins with respect to both osseointegration and bone-implant interface biomechanics and thus may improve primary stability and advance fracture fixation.

ZUSAMMENFASSUNG

HINTERGRUND: Sowohl Titan als auch diverse bioresorbierbare Polymere finden derzeit Anwendung als Osteosynthesematerial. Titan-Implantate müssen jedoch insbesondere in der Kindertraumatologie häufig in einer Zweitoperation entfernt werden und können „Stress-Shielding“ verursachen. Bioresorbierbare Polymere hingegen rufen gelegentlich Fremdkörperreaktionen hervor und weisen limitierte mechanische Eigenschaften auf. Ein neu entwickeltes Implantat aus einer völlig neuartigen bioresorbierbaren Magnesium-Legierung soll die oben genannten Nachteile überwinden und die hervorragenden mechanischen Eigenschaften metallischer Implantate sowie die Bioresorbierbarkeit von Polymeren verbinden.

METHODIK: Im Rahmen dieser Studie wurden glatte, unbeschichtete, zylindrische Implantate aus 3 verschiedenen Materialen (neu entwickelte bioresorbierbare Magnesium Legierung, neues bioresorbierbares PLGA-Polymer und herkömmliches Titan) hinsichtlich Osteointegration und Knochen-Implantat-Grenzflächenfestigkeit verglichen. Zu diesem Zweck wurden die Pins transkortikal in die femorale Diaphyse von 108 Sprague-Dawley Ratten implantiert und nach 1, 3 oder 6 Monaten mittels mikro-CT, pushout-Test und Fluoreszenzmikroskopie evaluiert. Zudem wurden die biomechanisch getesteten Implantate lichtmikroskopisch und exemplarisch auch elektronenmikroskopisch untersucht.

ERGEBNISSE: Die biomechanischen Tests ergaben hochsignifikant höhere mediane Maximallast und Scherfestigkeit dieser neuartigen Implantate im Vergleich zu PLGA- und Titan-Pins. Die mikro-computertomographisch bestimmte mittlere Knochen-Implantat Kontaktfläche dieser Magnesium-Implantate war ebenfalls signifikant größer als jene von Titan-Implantaten nach 1 und 6 Monaten sowie als jene von PLGA Implantaten nach 1 Monat.

ZUSAMMENFASSUNG: Wir konnten in dieser Studie zeigen, dass diese neuartigen bioresorbierbaren Magnesium-Implantate neuen PLGA und sogar herkömmlichen Titan-Implantaten hinsichtlich Osteointegration und Knochen-Implantat-Grenzflächenfestigkeit im Rattenmodell deutlich überlegen sind.

1 INTRODUCTION

1.1 AIMS AND HYPOTHESES

The aim of this experimental study was to evaluate the bone-implant interface biomechanics and osseointegration of two new biodegradable implants in comparison to conventional titanium pins in a transcortical rat model. To this purpose pushout testing, microfocus computed tomography, fluorescent labelling, light-microscopic and exemplary scanning electron microscopic examination of the tested implants were performed after an implantation period of 1, 3 as well as 6 months.

The first device investigated was a completely new type of biodegradable implant made of a magnesium alloy (henceforth referred to as Mg implant). This pin was supposed to combine excellent strength retention properties of metallic implants with biodegradability of polymers already used for fracture fixation. The second implant was a novel bioabsorbable pin made of poly(lactic-co-glycolic acid) (PLGA; lactide-to-glycolide ratio of 80:20) with new polymer orientation (henceforth referred to as PLGA implant). The third implant tested in the present study was a conventional pin of commercially pure titanium (Tn implant) which served as control.

Our project intends to test the following hypotheses:

- The biomechanical properties of the bone-implant interface (Biomech) (i.e. maximum pushout force, maximum shear strength, interface stiffness and energy absorption to failure) of Mg implants are equal or superior to those of Tn implants.

$$H_1 : \mu_{\text{Biomech}\,Mg} \geq \mu_{\text{Biomech}\,Tn}$$
$$H_0 : \mu_{\text{Biomech}\,Mg} < \mu_{\text{Biomech}\,Tn}$$

- The biomechanical properties of the bone-implant interface (Biomech) (i.e. maximum pushout force, maximum shear strength, interface stiffness and energy absorption to failure) of PLGA implants are equal or superior to those of Tn implants.

$$H_1 : \mu_{\text{Biomech}\,PLGA} \geq \mu_{\text{Biomech}\,Tn}$$
$$H_0 : \mu_{\text{Biomech}\,PLGA} < \mu_{\text{Biomech}\,Tn}$$

- Osseointegration (OI) exhibited by Mg implants is equal or superior to that of Tn implants evidenced by three parameters obtained by quantitative micro computed tomography (bone volume per total tissue volume (BV/TV), mean trabecular thickness (Tb.Th) and bone-implant contact area (BIC)).

$$H_1 : \mu_{OI\,Mg} \geq \mu_{OI\,Tn}$$
$$H_0 : \mu_{OI\,Mg} < \mu_{OI\,Tn}$$

- Osseointegration (OI) exhibited by PLGA implants is equal or superior to that of Tn implants evidenced by three parameters obtained by quantitative micro computed tomography (bone volume per total tissue volume (BV/TV), mean trabecular thickness (Tb.Th) and bone-implant contact area (BIC)).

$$H_1 : \mu_{OI\,PLGA} \geq \mu_{OI\,Tn}$$
$$H_0 : \mu_{OI\,PLGA} < \mu_{OI\,Tn}$$

- Analysed blood parameters (BP) of sacrificed rats which received Mg implants do not significantly differ from those of animals implanted with Tn implants, which indicates that these new implants do not induce a systemic inflammatory reaction.

$$H_1 : \mu_{BP\,Mg} = \mu_{BP\,Tn}$$
$$H_0 : \mu_{BP\,Mg} \neq \mu_{BP\,Tn}$$

- Analysed blood parameters (BP) of sacrificed rats which received PLGA implants do not significantly differ from those of animals implanted with Tn implants, which indicates that these new implants do not induce a systemic inflammatory reaction.

$$H_1 : \mu_{BP\,PLGA} = \mu_{BP\,Tn}$$
$$H_0 : \mu_{BP\,PLGA} \neq \mu_{BP\,Tn}$$

All evaluations were carried out after an implantation period of 1, 3 as well as 6 months.

1.2 OVERALL IMPORTANCE AND SIGNIFICANCE

During the past years the number of osteosynthesis in trauma patients, especially in children, constantly increased. The reasons for this are reduced duration of inpatient treatment and the possibility of functional after-treatment with early mobilisation and weight bearing – both resulting in reduced absence from school or work.

Up to now various metal implants, mainly stainless steel or titanium were used for implant design. Here the major disadvantage lies in a second operation, usually in general anaesthesia, which is necessary for implant removal. Additionally the rigidity of solid intramedullar metal implants protects bones from stress and thus may induce a mild osteoporosis [67]. These known disadvantages lead to the introduction of bioabsorbable implants. The major advantage of these implants is that removal becomes unnecessary [51,67] allowing early return to school or work and reduced duration of inpatient treatment. Additionally biodegradation of the implant is more compatible to fracture healing than rigid fixation with metal implants (with increasing degradation of the implant the stress is subsequently transferred to the bone leading to a stimulation by dynamic loading processes) [1,28,108,125]. Regarding the economical aspect a study comparing the costs of metal and biodegradable implants in selected fractures revealed a clear advantage of degradable implants [16]. However, the currently available bioabsorbable implants lack strength and stiffness [28,108], moreover associated inflammatory reactions and osteolysis have been reported [15].

Our experimental study evaluates a newly developed innovative type of biodegradable implant made of a magnesium alloy. This novel material is supposed to combine excellent strength retention properties of metallic implants with biodegradability of polymers already used as implant material. Furthermore it is expected to exhibit superior biocompatibility and bone-implant integration.

Therefore, the results of our study may lead to a further increase of biodegradable implants in (pediatric) orthopaedic trauma surgery leading to personal and socioeconomic benefits.

1.3 BACKGROUND

Bioabsorbable implants are implants made of biomaterials that degrade in vivo whereas the produced degradation fragments are introduced into normal physiologic and biochemical processes [27]. The vast majority of the clinically used biodegradable fixation devices are based on poly(glycolic acid) (PGA), poly(lactic acid) (PLA) and their co-polymers. The hydrolytical scission is the prevailing mechanism of polymer degradation [44,73] in these polymers which are finally degraded to carbon dioxide and water via citric acid cycle. The terms “bioabsorbable” and “biodegradable” will be used synonymously in this thesis.

1.3.1 Biodegradable Polymeric Implants – Assets and Drawbacks

The main assets and drawbacks of biodegradable polymeric implants will be outlined in the following sections:

1.3.1.1 Assets

There are two chief advantages of biodegradable polymer implants:

First, contrary to metal alloys most commonly used in fracture-fixation devices bioabsorbable implants obviate the need for a second surgical intervention for implant removal. Thus an additional risk of anaesthesia and infection is eliminated and further inpatient treatment as well as varying periods of disability generally associated with such a retrieval operation can be prevented. Hence, the use of degradable implants is particularly appealing in paediatric trauma surgery [99] where implant removal is exceedingly frequent.

Second, absorbable fracture fixation devices have overcome another significant drawback of metal implants: Metal devices retain a large portion of the mechanical load applied to the bone because of their high Young´s modulus compared to bone. This phenomenon called “stress shielding” may result in bone resorption and implant loosening [34,108]. Unlike metal implants bioabsorbable devices ensure adequate initial stability for fracture consolidation, transfer increasing load to healing bone as they gradually degrade and thus lead to stimulation of the healing

process by dynamic loading [27,73,125] .

Besides, there are other advantages that deserve mentioning: Biodegradable implants facilitate postoperative radiologic imaging as they do not cause artefacts in magnetic resonance imaging and computer tomography in contrast to metallic devices [108]. Furthermore studies analysing the financial implications of the use of absorbable implants revealed a clear (removal rate dependant) advantage of degradable implants in selected fractures [12,16]. Moreover, potential corrosion, wear and debris formation of retained metal implants can be avoided [44]. Biodegradable fracture fixation devices may also be an option in patients confronted with problems of sensitivity to metal components of the implants, especially nickel.

1.3.1.2 Drawbacks

Since their initial inauguration, several drawbacks and limitations of absorbable fracture fixation appliances have been reported:

First, after clinical implementation of absorbable internal fracture fixation devices it became obvious that these devices sometimes induce adverse tissue reactions [15,19]. Histopathological analyses revealed a rather uniform nonspecific inflammatory, abacterial foreign-body reaction that could be observed even in patients without any clinically manifest inflammatory reaction [11]. Scores of macrophages and foreign-body giant cells phagocytosing polymer degradation particles as well as neutrophilic leucocytes and lymphocytes were seen. On the contrary polyglycolide was found to be an immunological inert implant material in human lymphocyte cultures [93]. In most cases this tissue response takes place without any clinical symptoms, but in some patients the inflammatory foreign-body reaction becomes manifest. Böstman et al. [15] described the clinical characteristics of this tissue response: Initially an erythematous, fluctuating and painful papule arises over the implant track and bursts open within a few days resulting in a sterile sinus discharging liquid degradation remnants. Radiologically osteolytic lesions along the implant track are present in about 50% of these patients [18,41]. Consequently classification systems have been established to be able to compare adverse tissue response reported in different clinical studies [50,117]. Moreover, it has been shown that the inci-

dence of foreign-body reactions to biodegradable implants is independent of the implant volume as well as of the age and gender of patients [11,19]. However screw shape of implants (compared to cylindrical shape) and poor vascularity (as in case of scaphoid bone) seem to increase tissue response rate [19]. Böstman [15] et al. hypothesised that this may be due to a insufficient clearing capacity of these tissues resulting in a local accumulation of polymeric degradation remnants. In a survey including a total of 2500 patients having bioabsorbable implants for internal fixation Rokkanen et al. [91] noted a nonspecific foreign body reaction rate of 2.3% and an implant failure rate of 3.7%. In 2528 patients operated on using polyglycolid and polylactid implants Böstman et al. [19] reported a clinically significant foreign body reaction in 0.2% and 5.3%, respectively. The incidence of this adverse tissue reaction varied from 1.8% (radial head fracture) to 25% (ununited fractures of the scaphoid) according to fracture site and was observed 11 weeks postoperatively on average. Besides, synovial inflammation after intra-articular fixation [15] and moderate to severe osteoarthritis of the ankle after prior foreign-body reactions [17] have been described. Consequently, the author of the latter article recommended to avoid absorbable implant placement near joint spaces because an inflammatory foreign-body reaction may lead to intraarticular dissemination of polymeric degradation remnants resulting in osteoarthritic changes.

Second, mechanical properties of biodegradable fracture fixation devices are limited even though their strength has been improved particularly by self-fibre-reinforcement [105]. However, moduli (especially modulus of elasticity) of these biomaterials could not be increased sufficiently yet [28]. In addition, loosening of biodegradable polymeric fixations often occurs due to creep and relaxation, which are characteristic properties of these materials [28]. Consequently, absorbable implants have found applications where lower-strength materials are sufficient (such as in the hand, foot and ankle as well as soft tissue fixation) but are not yet suitable for fractures of load bearing cortical bone where they might fail due to excessive mechanical stress [28,108].

The main assets and drawbacks of biodegradable implants are summarised in Table 1-1.

Table 1-1. Synopsis of main assets and drawbacks of biodegradable implants in orthopaedic trauma surgery

Assets	Drawbacks
No need for implant removal	Adverse tissue reactions
No „stress shielding“	Limited mechanical properties
Gradually load transfer to bone	Invisibility in postoperative x-ray examination
Cost effectiveness	
Facilitate postoperative MRI and CT evaluation	

1.3.2 Current clinical role of biodegradable implants

The use of bioabsorbable implants in trauma and bone surgery became more frequent during the last years. Polymers made from lactic acid (PLA), glycolic acid (PGA), and dioxanone (PDS), as well as their copolymers (e.g., poly(lactic-co-glycolic acid) (PLGA)), are most frequently used and readily available as implants for both bone and soft-tissue fixation [34]:

Various implants made of bioabsorbable materials were used clinically with increasing frequency for fixation of tendons and ligaments to bone in arthroscopic surgery and sports medicine [2,28,47]. Several screws, arrows, tacks, suture anchors and sutures have been developed and evaluated for meniscal repair [9,87,106], anterior cruciate ligament reconstruction [39,57,107,126] and treatment of shoulder lesions [25,116].

Furthermore, biodegradable fixation devices of various kinds were applied for fracture treatment especially in craniofacial and orthopaedic trauma surgery [44,108]. Fractures of the foot and ankle have been a main field of application: Bucholz et al. [24] found no statitistically significant differences in radiographic and functional results as well as complication rates when comparing medial malleolar fixation with use of either PLA-screws or stainless-steel screws in 155 patients who had a

closed, displaced medial malleolar, bimalleolar, or trimalleolar fracture of the ankle. Pelto-Vasenius [84] cited a redisplacement rate, foreign-body reaction and infection rate of 2.5%, 9.0% and 3.6%, respectively, after operative treatment of 1202 fractures of the ankle by means of absorbable implants (implant materials: PGA/PLA-copolymer, self-reinforced PGA and self-reinforced PLLA) during a 10-year period. After treatment of intra-articular calcaneal fractures in 21 patients within a prospective clinical study Kankare et al. [60] concluded that outcome was similar to those treated with other operative methods. Similar results were found for displaced fractures of the neck or body of the talus [62] and selected tibial condylar fractures [61]. Sinisaari et al. [98] demonstrated that there were no significant differences between the patient groups in any of the clinical and radiological parameters measured after surgical treatment of ruptured tibio-fibular syndesmosis with either metallic or bioabsorbable self-reinforced poly-L-lactide screws. Moreover good clinical results could be achieved after refixation of osteochondral fragments of the ankle and knee joints using self-reinforced absorbable pins, nails and screws made of PLA [42]. In addition bioabsorbable fixation is a worthwhile option in large osteochondral fractures of the lateral femoral condyle in the adolescent [114]. Biodegradable implants were also applied for fixation of femoral head fractures associated with a traumatic dislocation of the hip [55] as well as for the treatment of femoral fractures involving the physeal plate [79]. Excellent results have been reported after internal fixation of displaced radial fractures [49,85] and fractures of the olecranon [78] using absorbable pins and/or screws. Moreover bioarbsorbable fracture fixation devices have been adopted for fractures, osteotomies and fusions of the hand [52,115]. Besides, Fedorowicz et al. [38] statet no statistically significant difference in postoperative discomfort, patient satisfaction and infection using either titanium or biodegradable materials in orthognathic surgery.

In paediatric trauma surgery bioabsorbable fracture fixation is particularly appealing because it abolishes the need of implant removal. Hope et al [51] could verify identical clinical results in long-term follow-up of children (mean age 8 years) after stabilisation of elbow fractures (medial or lateral condyle respectively olecranon) with either metal Kirschner-wires or biodegradable pins (prospective randomised trial). Furthermore Eppley et al report excellent results after craniofacial surgery of

one-hundred 4-15 months old children with biodegradable implants (LactoSorb®) [37] and found no long-term implant-related complications in any patient after treatment of 44 pediatric facial fractures using different degradable bone fixation devices [36]. In experimental studies, the presence of an absorbable implant did not affect the growth plate any more than an empty drill hole does [69]. In addition, in a clinical study by Böstman [14] transphyseal self-reinforced polyglycolide pins did not cause signs of impairment of physeal function with follow-up times up to 10 months. In a prospective study including 71 paediatric patients with physeal or nonphyseal fractures Böstman et al. [13] compared self-reinforced PGA-pins and conventional Kirschner wires (mean follow-up interval of 15.8 months, mean age of the patients: 9.8 years (range 2-15 years)): In 87% of fractures adequate anatomic reduction could be maintained until union. Böstman concluded that the results of fracture fixation using biodegradable polyglycolide pins had been satisfactory except for supracondylar humerus fracture (in 6 of 14 patients displacement of fracture position ocurred), which may be due to the higher displacement forces in these fractures. Moreover Mäkelä et al. [68] reported excellent results in the treatement of distal humeral physeal fractures using transphyseal biodegradable fixation (self-reinforced PGA- pins): All 19 children showed good results and secondary displacement or signs of growth disturbance were seen in none of them during a mean follow-up period of 17.2 months. However, there is still a lack of carefully controlled randomized prospective trials that analyse the efficacy of biodegradable implants in treating particular fracture patterns.

1.3.3 Biomechanical Testing of the Bone-Implant Interface

A main goal of implant-related research in orthopaedic trauma surgery is to achieve sufficient fixation and anchoring of the implant in the surrounding bone by direct apposition or ingrowth of newly formed bone to the implant surface without an intervening soft tissue layer (=osseointegration) [31,40,70,111]. Hence, several biomechanical test methods have been developed for the mechanical evaluation of bone-implant integration and for the assessment of interfacial bonding strengths: Pushout or pullout tests [7], torque tests [21-23] and tensile tests [75]. Since pushout test-

ing is most commonly used and was also chosen for this experimental study, it will be delineated in the following sections:

1.3.3.1 Pushout Test

Pushout tests have been adopted for various purposes in implant-related orthopaedic and dental research, but were mainly utilised to evaluate effects of implant material, implant geometry, implant surface configurations and coatings on osseointegration and interfacial bonding [72].

In general, the following procedure has to be passed through for pushout testing: Cylindrical implants, typically used for this purpose, are implanted into cortical or less frequently in trabecular bone at the favoured anatomical site of several experimental animals in vivo. After the implants have been left in situ for the designated implantation period, the animal is sacrificed and the bone implant specimen is retrieved. Thereafter, the harvested bone-implant sample is tested freshly immediately after sacrifice or it is frozen and tested after thawing at a later date. After preparation of the sample for biomechanical analysis it has to be properly placed and accurately aligned to the support jig. Finally, the load is applied until implant failure at a constant displacement rate via a push rod connected to the crosshead of the materials testing machine. It is important to note that the load has to be transferred strictly axially, so that the line of action of the loading force is collinear with the long axis of the implant [33]. Load and displacement are recorded during pushout testing resulting in an load-displacement curve:

1.3.3.1.1 Load-Displacement-Curve

Load-displacement curves resulting from pushout testing typically show the applied load [N] along the axis of ordinate and the displacement of the implant in the surrounding tissue along the horizontal axis of abscissae. With regard to this curves, several well established parameters may be determined to characterise the biomechanical properties of the bone-implant interface:

The **Maximum Pushout Force (F_{max})** [N] (also referred to as “peak force”, “ultimate load” or “interface shear modulus”) represents the recorded peak force pro-

voking failure of the bone-implant interface, which may be discerned as abrupt displacement of the implant within the surrounding bone.

The **Ultimate Shear Strength** of the Interface **(σ_u)** [N/mm^2] (also referred to as "maximum shear stress" or "ultimate shear stress") is calculated by dividing the maximum pushout force (F_{max}) by the actual bone-implant contact area (BIC), since F_{max} has to be related to the actual BIC (also referred to as "nominal interface area") for the sake of comparability of different bone-implant specimens:

$$\sigma_u = F_{max} / BIC$$

Dhert et Jansen [33] noted that σ_u is composed of various fixation modes such as friction, mechanical interlock and chemical bonding.

Interface stiffness [N/mm] (also referred to as "apparent shear stiffness", "apparent shear modulus" or "interface shear modulus") is measured as the slope of the load-displacement curve in its linear region or may be calculated as F/d or (F/BIC)/d, where `F´ is the applied load [N], `BIC´ is the bone-implant contact area [mm] and `d´ is the displacement [mm].

Energy absorption to failure [Nmm = mJ] represents the energy delivered until the bone-implant interface fails and is determined as the area under the load-displacement curve until failure (i.e., maximum pushout force).

1.3.3.1.2 Comparability and Validity of Pushout Tests

It is quite obvious that pushout data indicates the extent of implant anchorage in the surrounding bone and thus provides essential information for the clinical practice. However, it has been illustrated that pushout test results widely vary and may hardly be compared between different investigators due to variations in methods of pushout testing [33]. In consequence of this lack of comparability and since no consensus standard pushout test method has been established yet, Black [8] postulated that the pushout test design and test conditions have to be described and specified in detail. In addition, Black listet implant-specific (implant dimensions, surface geometry and composition), host-specific (species, age, implantation site) and other factors (tissue handling after sacrifice, intraoperative fit, alignment and

mounting, fit of the support jig, mode of failure, true interfacial surface area) which may affect the results of pushout tests and thus should be mentioned in future reports. Besides, Dhert [33] stressed the importance of failure mode analysis: It has to be clarified whether the failure had occurred within the trabecular bone, at the bone-implant interface or at the coating-substrate interface (if coated implants were used) in order to prevent comparing the mechanical properties of completely different structures.

1.3.3.1.3 Crucial Test Conditions of Pushout Tests

As mentioned above, proper alignment among the push rod, the specimen and the support jig as well as load transfer collinearly to the long axis of the implant are crucial with regard to valid pushout test results [33]. Furthermore, several authors investigated the potential influence of various test conditions on pushout test data by means of finite element analyses: Usually, the maximum pushout force is divided by the actual bone-implant contact area resulting in ultimate shear strength which in turn is supposed to typify the interfacial bonding strength. This simply division for shear strength/shear stress calculation is based on the assumption that stress distribution is uniform at the bone-implant interface and yields the bond strength only in an average sense which may significantly differ from the real value [33]. However, Harrigan et al. [48] revealed that the stress distribution along the interface is irregular with high stresses particularly in the region between the base of the specimen and the support jig. Thus, he concluded to rather compare failure loads than interface shear strength/interface shear stress of tested specimens. Moreover, these specimens have to be of very similar geometry and should be tested under identical loading conditions. Furthermore Dhert et al. [32] could show that the clearance of the hole in the support jig (interface stress distribution becomes more uniform when the clearance is increased) and Young´s modulus of the implant (low Young´s modulus causes less uniform stress distribution) were of major impact for the occurrence of peak stresses at the interface, whereas cortical thickness (implant length) and implant diameter can be neglected. Hence, he advised that the clearance of the hole in the support jig should be at least 0.7 mm and that tested implants have to be of similar Young´s modulus. Shirazi-Adl [95,96]

demonstrated that interface stress distribution may also be influenced by relative material properties, boundary conditions and initial interference.

1.3.4 Use and Limitations of Microfocus Computed Tomography for the Assessment of Bone-Implant Integration

Due to high spatial resolution up to 1 µm and high image contrast histomorphometric analysis of thin histologic sections is considered as gold standard for investigating trabecular bone structure, bone healing and bone remodelling around implants. However, required sample preparation is exceedingly time-consuming, may cause artefacts and yields only few two-dimensional sections whereas considerable amount of material is lost [35]. Moreover, the destructive nature of this procedure precludes any subsequent analysis such as biomechanical testing.

Microfocus computed tomography (µCT) is a relative new imaging modality and may overcome some of these limitations. This technique has the potential to improve the morphologic evaluation of the bone-implant interface as it provides full three-dimensional data and allows for two-dimensional image reconstruction in an arbitrary plane. Furthermore, it is non-destructive, less time-consuming and provides a spatial resolution up to 5 µm [35]. Therefore, this emerging technique has attained great interest in the field of orthopaedic and small animal research [35,80].

Bone structural parameters were found to be highly correlated between microcomputed tomography and conventional histomorphometry. Thus, µCT could be validated as method for the assessment of trabecular [64,74,104] as well as cortical bone [5].

Furthermore, several authors evaluated the capability of microfocus computed tomography for the assessment of peri-implant bone and osseointegration:

Van Oosterwyck et al. [109] compared 6 histological sections of one bone-implant specimen (titanium implant; Skyscan 1072 µCT scanner, resolution of 60 µm) with the corresponding µCT slices. This qualitative evaluation showed that the overall trabecular structure obtained by both techniques is very similar even very close to the bone-implant interface. Moreover the titanium implant did not produce any

substantial artefacts. Kiba et al. [63] could clearly detect bone-implant contact, soft tissue, trabecular structure of newly formed bone and areas of bone resorption corresponding to histologic examination when analysing 4 dental bone-implant samples by means of µCT (SMX-225CT, Shimadzu). No artefacts were seen. Butz et al. [26] determined the ratio of bone area to total area in defined zones at the bone-implant interface of 2 specimens with use of micro-computed tomography and histomorphometry. Correlation between these techniques was significant for cancellous ($r = 0.92$, $p < 0.05$) as well as cortical ($r = 0.65$, $p < 0.05$) bone at distances of 24 to 240 µm from the surface of the unthreaded cylindric titanium implant. But in closer proximity (0 to 24 µm from implant surface) no significant correlation could be detected which may be caused by metal artefacts, as presumed by the author. Rebaudi et al. [88] cited similar bone-to-implant apposition in 1 human sample containing a titanium micro-implant when measured by µCT (microCT20, Scanco) as well as histomorphometry. In consequence of metal artefacts Stoppie et al. [101] could not detect bone in a region 60 µm or closer to the titanium implant surface when comparing 150 histologic sections (obtained from 6 bone-implant specimens) with the corresponding µCT slices (Philips HOMX 161 microfocus x-ray system, isovoxel size: 24 µm). However, overall matching and overall Spearman´s correlation between the bone area data of these two techniques were 89.23% and 0.86, respectively. Besides, this group [102] examined the value of in-vivo microfocus computed tomography for the assessment of peri-implant bone and described considerable lower agreement between histological and µCT measurements.

Furthermore, it has been emphasised that synchrotron x-ray tomography may be more suitable for the evaluation of bony tissue at the bone-implant interface than micro-computed tomography [6,56]. However, this imaging modality is very expensive, time-consuming and hardly available. Thus it is not practicable for experimental studies including scores of animals.

In summary, micro-computed tomography seems to be a reliable tool for peri-implant bone measurement with some potential limitations in close vicinity of the implant surface.

1.3.5 Effects of Cryopreservation on the Biomechanical Properties of Bone and Bone-Implant Specimens

Biomechanical testing of freshly retrieved specimens immediately after sacrifice is often not feasible for organisational reasons. For example, in the present study it was all but impossible to perform µCT-imaging and biomechanical testing within few hours of harvesting. Consequently, frozen storage is frequently used to preserve fresh samples until testing.

Yet, it is of utmost importance to ensure that the biomechanical properties of the tested cadaveric bone-implant specimens reflect the in vivo properties of the harvested fresh specimens in order to increase validity of the biomechanical tests. Hence, we reviewed literature and chose a storage method which is not supposed to significantly affect the biomechanical properties of the bone-implant interface of our specimens:

Many studies have been performed focusing on the influence of various preservation and sterilization methods on the biomechanical behavior of bone. According to the literature, storage in 10% formalin [45,118], freeze-drying [58,83,97] and storage in ethanol [113] significantly alter the mechanical properties of bone; and so do high-dose irradiation [113], chemical sterilization [90], chemical sterilization and partial decalcification [90], ethylene oxide sterilization [54,90], boiling [10] and autoclaving [10,113]. In contrast to these procedures, cryopreservation does not seem to affect the biomechanical properties measurably (Table 1-2) if the moisture of the samples is preserved and is therefore frequently used to storage fresh bone specimens until biomechanical testing is performed.

Although many authors investigated the biomechanical effects of freezing on bone tissue, there seems to be a lack of data on the influence of cryopreservation on the biomechanical properties of the bone-implant interface: To the best of the author´s knowledge, only one study dealing with this subject has been published: Huss and coworkers [53] investigated the influence of freezing temperature and storage duration on the pullout force of transcortically inserted Steinmann pins: 16 femurs of 8

dogs were harvested immediately after euthanasia and 80 unthreaded Steinmann pins (5 pins/femur) were inserted into the diaphysis perpendicular to the long axis of the femurs within 15 minutes of sacrifice. Subsequently each femur was transected using a band saw resulting in 5 bone-implant specimens per femur. These specimens were evenly distributed to 5 groups: group 1: tested within 4 hours of harvesting (= control group); group 2 and 4: cryopreservation at -20°C ± 5°C for 14 and 28 days, respectively; group 3 and 5: cryopreservation at -70°C ± 2°C for 14 and 28 days, respectively. A pullout test was performed and maximum pullout force was determined: Comparing the mean maximum pullout forces of the different groups no statistically significant difference among any of the groups could be found. Thus, neither cryopreservation temperature nor storage duration had a statistically significant effect on pin pullout force. However, specimens preserved at -20°C showed a tendency towards increased maximum pullout forces compared to the specimens of the control group. Therefore, Huss suggested to cryopreserve bone-implant specimens at -70°C if possible. Besides, using headspace gas chromatography Laitinen et al. [65] could show that the extent of lipid oxidation in 84 bone samples (obtained from 21 femoral heads) was influenced by storage temperature and storage duration: The speed of lipid oxidation and hence the concentration of volatile oxidation products was significantly higher at -30°C than at -70°C (the concentration at -70°C was near the detection limit). Due to the potential impairment of bone quality by these byproducts of oxidation (which is not clear yet) he recommended to preserve bone allografts at -70°C or lower, whereas Pereira et al. [86] reported cortical hairline cracks after cryopreservation of 25 whole canine femurs at -70°C as well as -150°C resulting in a massive loss of torsion strength.

However, numerous studies could not find a significant alteration of the mechanical properties despite different freezing temperatures and storage periods (see Table 1-2: [10,45,58,71,77,86,90]) and thus it is questionable if this lipid oxidation is of relevance to the biomechanical properties of bone. Since several freezing temperatures ranging from -20°C to -196°C have been shown to not influence the mechanical properties of bone (see Table 1-2: [71,77]), most authors cryopreserve their specimens at -20°C until mechanical testing due to practical considerations.

Furthermore, Voggenreiter et al. [112] found no alterations of the surface structure of cryopreserved cortical bone from rat tibiae (frozen at -70°C for 28 days) using scanning electron microscopy. Salai et al. [92] noted that there were no qualitative histological differences between human proximal humeral bone allografts frozen at -80°C up to 5 years and freshly controls. Moreover, it has been shown that several freeze-thaw cycles do not significantly affect the mechanical parameters of bone [10,59,66] and Kääb et al. could not find significant changes in pullout strengths of cancellous screws inserted into 48 thawed human cadaveric vertebral bodies throughout a 3.5 day testing period.

Several authors pointed out that cryopreserved samples have to be sealed tightly in order to preserve their moisture and prevent dehydration which may affect their mechanical behaviour [46,54,77].

In consideration of the literature reviewed, cryopreservation of freshly harvested and tightly sealed specimens at -20°C does not seem to affect their mechanical properties, which is of utmost importance with regard to the validity of biomechanical testing.

Table 1-2: Influence of cryopreservation on the biomechanical properties of bone (References cited in chronological order)

Reference	Bone Samples	Storage Condition	Results
[83]	90 rat femurs and 324 rat tail vertebrae	• -20°C for 2 weeks *(femurs: n= ND; vertebrae: n=72)*, • -70°C for 2 weeks *(femurs: n= ND; vertebrae: n=75)* and • -196°C for 2 weeks *(femurs: n=ND; vertebrae: n=54)*; • Freshly tested specimens *(femurs: n= ND; vertebrae: n=55)*,	Torsion tests of femora: No statistically significant difference in torque to failure and energy to failure compared with fresh tested controls; specimens stored at -196°C showed a statistically significant increase of angular deformation at failure and a statistically significant decrease of torsional stiffness. Compression test of vertebrae: specimens storaged at -20°C and -70°C showed a sligthly (but statistically significant) increase of stress at failure and of elastic modulus compared with freshly tested controls; Storage at -196°C caused a statistically significant increase of stress at failure, strain at failure and energy absorption to failure.
[77]	8 human thoracic functional spine units	• -18°C for 21 days *(n=2)* and • -18°C for (averaged) 193 days *(n=4)*; • Freshly tested specimens *(n=2)*	Biomechanical properties of fresh cadaveric functional spine units were not significantly affected by frozen storage up to 232 days.
[90]	Femora of adult dogs *(one femur of each dog was tested freshly and served as the matched control)*	• -20°C for 1 week *(n=5)*, • -20°C for 16 weeks *(n=5)* and • -20°C for 32 weeks *(n=5)*; • Freshly tested specimens *(n=5/group)*	Screw pullout load and screw stripping torque: no statistically significant differences for all 3 storage periods compared with the freshly tested matched controls; Compressive load to failure of a whole diaphyseal segment: -20°C for 1 week: statistically significant increase; -20°C for 16 and 32 weeks respectively: no statistically significant differences compared with the freshly tested matched controls
[45]	Humeri and femora of 48 adult cats *(left bones were tested freshly and served as matched controls)*	• -20°C for 3 days (*n= ND)* and • -20°C for 21 days (*n= ND)*; • Freshly tested specimens (*ND)*	Freezing did not alter the mechanical properties evaluated in a torsion test (humeri) and in a four-point bending test (femora) compared with the untreated, immediately tested contralateral control bones.

[66]	Cylindrical trabecular bone specimens from the proximal tibial epiphysis of 2 male amputees *(the fresh specimens were tested nondestrucively, storaged and tested again)*	• -20°C for 1 day *(n=19)*, • -20°C for 10 days *(n=18)* and • -20°C for 100 days *(n=19)*; • Freshly tested specimens *(n=19, n=18 and n=19, respectively)*	Nondestructive compression test: storage by freezing did not alter the stiffness, elastic energy and hysteresis energy; loss tangent increased statistically significant with storage duration.
[10]	Cylindrical trabecular bone specimens obtained from 3 bovine humeri	• -20°C for 8 days *(n=24)*, • -70°C for 8 days *(n=24)* and • 8 freeze-thaw cycles at -20°C in 8 days (1 cycle per day) *(n=24)*; • Freshly tested specimens *(n=24)*	Compressive modulus and compressive strength of the cryopreserved specimens did not differ significantly compared with the untreated, immediately tested control group
[46]	11 pairs of metacarpal and 10 pairs of metatarsal bones and 7 pairs of ribs from 4 adult dogs *(one bone of each pair was randomly allocated to the first treatment, the contralateral one to the second)*	• Immersed in physiological saline at -20°C for 1 year *(metacarpal bones: n=11; metatarsal bones: n=10; ribs: n=7)* vs. • Packaged in plastic at -20°C for 1 year *(metacarpal bones: n=11; metatarsal bones: n=10; ribs: n=7)*	Torsion test: no significant difference 4-point bending test: displacement at failure and energy absorbed at failure were significantly greater in case of immersion (increase of 25 to 30% and 18 to 24%, respectively); slope, displacement at yield point, bending moment at yield point and bending moment at failure: no statistically significant differences
[58]	Rat femurs and first tail vertebrae	• -80°C for 2 weeks *(n=10 specimen),* • -80°C for 6 weeks *(n=10 specimen)* and • -80°C for 12 weeks *(n=10 specimen)* • Freshly tested specimens *(n=10 specimen)*	3-point bending test (femurs): Cryopreserved femurs showed a mean 7.2% decrease in bending strength compared with the fresh control group. No statistically significant difference could be found between the 3 freezing periods. Compression test (vertebrae): Cryopreserved vertebrae showed a mean 11.0% decrease in compressive strength compared with the fresh control group. No statistically significant difference could be found between the 3 freezing periods.
[113]	Rat tibiae	• -70°C for 28 days *(n=8)*; • Freshly tested specimens *(n=8)*	Cryopreservation did not alter any of the biomechanical parameters tested in a 3-point bending test compared with fresh tested control bones

[86]	25 femurs of adult dogs	• -150°C for 3 months vs. • -70°C for 3 months	No statistically significant differences could be found between these 2 groups in a torsion test.
[92]	Human cortical bone specimens in the form of matchsticks obtained from the proximal humeral diaphysis (sourced through a bone bank) *(number of donors and number of tested specimens: ND)*	• -80°C for 3 years *(n= ND)* and • -80°C for 5 years *(n= ND)*; • Freshly tested specimens *(n= ND)*	Cryopreservation at -80°C for 3 years as well as for 5 years did not alter any of the biomechanical parameters tested in a 3-point bending test compared with fresh tested specimens.
[71]	155 standardized cancellous cylinders obtained from porcine humeral heads *(exact number of donor-animals: ND)*	• -20°C for 6 months *(n=20)*, • -20°C for 12 months *(n=23)* and • -20°C for 24 months *(n=20)*; • -80°C for 6 months *(n=20)*, • -80°C for 12 months *(n=20)* and • -80°C for 24 months *(n=20)*; • Freshly tested specimens *(n=32)*	A cancellous bone screw was inserted in each cancellous cylinder after thawing; thereafter a (screw-)pullout test was performed: none of the 6 groups showed any statistically significant difference with regard to the analysed maximum tensile strength compared with fresh tested controls.

ND = neither described nor discernible

2 MATERIALS AND METHODS

2.1 MATERIALS

2.1.1 Animals

108 Sprague-Dawley rats five weeks of age, weighing 120 to 140g were purchased from the Institute for Laboratory Animal Science and Genetics in Himberg (Core Unit for Biomedical Research, Medical University Vienna). During the experimental period the animals were housed in pairs under a 12:12 hours light-dark cycle in the animal laboratory of the Institute for Biomedical Research of the Medical University of Graz. Special forage for rats (Sniff®) and water were provided ad libitum. The animals were allowed to acclimatise to these conditions for one week prior to surgery. The animal experiments were approved by the Austrian Federal Ministry of Science and Research (approval number: BMDWK-66.010/0054-Brgd/2006) according to BGBl. I Nr. 162/2005.

2.1.2 Implants

In the present study, unthreaded uncoated smooth cylindrical-shaped pins designed by Synthes (Synthes Corporation, Oberdorf, Switzerland) were used. The first implant investigated was a completely new type of biodegradable implant made of a magnesium alloy (henceforth referred to as Mg implant). This pin was supposed to combine excellent strength retention properties of metallic implants with biodegradability of polymers already used as implant material. The second implant was a novel bioarbsorbable pin made of poly(lactic-co-glycolic acid) (PLGA with a lactide-to-glycolide ratio of 80:20) with new polymer orientation (henceforth referred to as PLGA implant). The third implant tested in the present study was a pin of commercially pure titanium (henceforth referred to as Tn-implant) which served as control.

All three implant types were of similar dimension and surface roughness (see Figure 2-2 and Table 2-1).

Figure 2-1. Macroscopical aspect of implant types used in the present study

Titanium implant *(left)*, Mg implant *(middle)* and PLGA implant *(right).*

The used pins solely differed in Young´s Modulus (nBM-Implant and titanium implant vs. PLGA implant) (Table 2-1).

Table 2-1. Implant specifications including dimension and Young´s Modulus

Implant Type	Diameter	Length	Young´s Modulus
Mg Implant	1,6 mm	7mm	110 GPa
PLGA Implant	1,65 mm	7mm	3 GPa
Titanium Implant	1,6 mm	7mm	45 GPa

Scanning electron micrographs of each implant type were recorded prior to implantation (Figure 2-2). These images served as controls and were compared to micrographs obtained from mechanically tested bone-implant specimens.

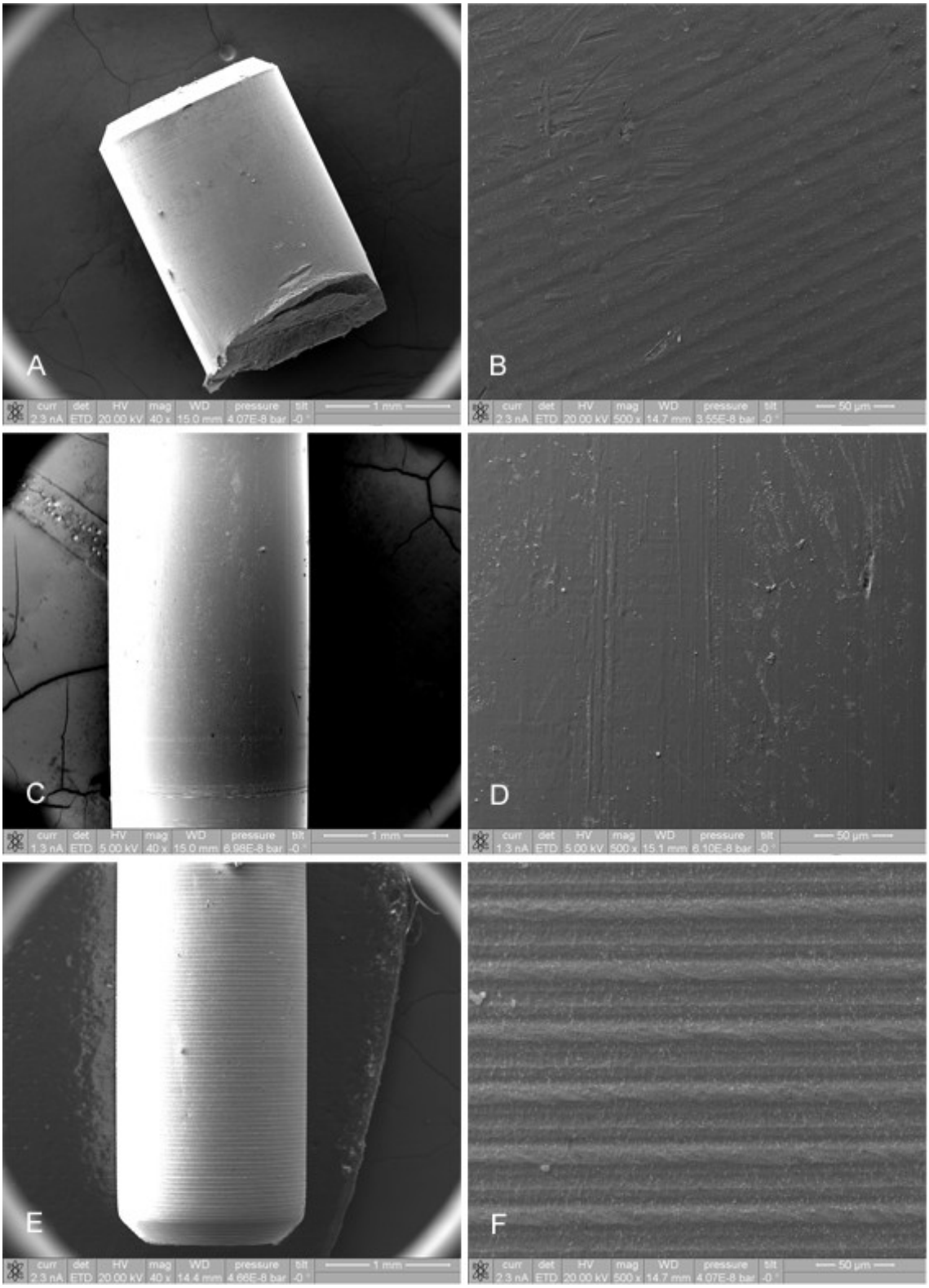

Figure 2-2. Scanning electron micrographs of implant types investigated in the present study

(A) Mg implant (original magnification x 40), **(B)** Mg implant (original magnification x 500), **(C)** PLGA implant (original magnification x 40), **(D)** PLGA implant (original magnification x 500), **(E)** titanium implant (original magnification x 40), **(F)** titanium implant (original magnification x 500).

2.1.3 Phamaceuticals

All pharmaceuticals used for anesthesia, antagonizing anesthesia, postoperative pain therapy and euthanasia, respectively, are given in the following tables.

Table 2-2. Pharmaceuticals used for anesthesia

Propriety Name	Generic Name	Particulars	Manufacturer
Fentanyl®	Fentanyl	50µg/ml	Janssen-Cilag GmbH, Neuss, Germany
Midazolam Delta®	Midazolam	1mg/ml	Deltaselect GmbH, Dreieich, Germany
Domitor®	Medetomedin	1mg/ml	Pfizer Corp. Austria GmbH, Vienna, Austria

Table 2-3. Pharmaceuticals used for antagonizing anesthesia

Propriety Name	Generic Name	Particulars	Manufacturer
Naloxon®	Narcanti	400µg/ml	Torrex Chiesi Pharma GmbH, Vienna, Austria
Anexate®	Flumazenil	100 µg /ml	Roche Austria GmbH, Vienna, Austria
Antisedan®	Atipamazol	5mg/ml	Pfizer Corp. Austria GmbH, Vienna, Austria

Table 2-4. Pharmaceuticals used for euthanasia

Propriety Name	Generic Name	Particulars	Manufacturer
Forane®	Isofluran		Abbot Laboratories Ltd., Kent, England
Thiopental Sandoz®	Thiopental	25mg/ml	Sandoz GmbH, Kundl, Austria

Table 2-5. Pharmaceuticals used for postoperative pain therapy

Propriety Name	Generic Name	Particulars	Manufacturer
Rimadyl®	Caprofen	50mg/ml	Pfizer Corp. Austria GmbH, Vienna, Austria
Novalgin® Drops	Metamizol	500mg/ml	Sanofi-Aventis GmbH, Vienna, Austria

2.1.4 Fluorochromes

Table 2-6: Fluorochromes

Propriety Name	Generic Name	Manufacturer
Oxitetrazyklin	Terramycin 100mg mit PVP®	Pfizer Corp. Austria GmbH, Vienna, Austria
Calcein blue	Calcein blue	Sigma-Aldrich Chemie GmbH, Munich, Germany
Xylenolorange	Xylenolorange	Sigma-Aldrich Chemie GmbH, Munich, Germany
Calcein	Calcein	Sigma-Aldrich Chemie GmbH, Munich, Germany

Calcein blue, Xylenolorange and Calcein were dissolved in 2.1% sodium bicarbonate, whereas Oxitetrazyklin was diluted in sodium chloride. Subsequently the solutions were filtrated sterilely.

2.1.5 Micro Computed Tomographer

Retrieved bone-implant specimens randomly allocated to the biomechanical testing group were analysed by high-resolution microcomputed tomography (micro-CT) using a VivaCT 75 system (Scanco Medical, Bassersdorf, Switzerland).

2.1.6 Mechanical Test Machine and Test Fixture

A self-engineered mechanical testing device (designed by Prof. Elmar Tschegg, Institute of Solid State Physics, Vienna University of Technology) was used for pushout testing of bone-implant specimens of group 1, 4 and 7. Samples of group 2, 3, 5, 6, 8 and 9 were mechanically tested with use of a materials testing machine with higher performance (RSA100, Carl Schenck AG, Darmstadt, Germany).

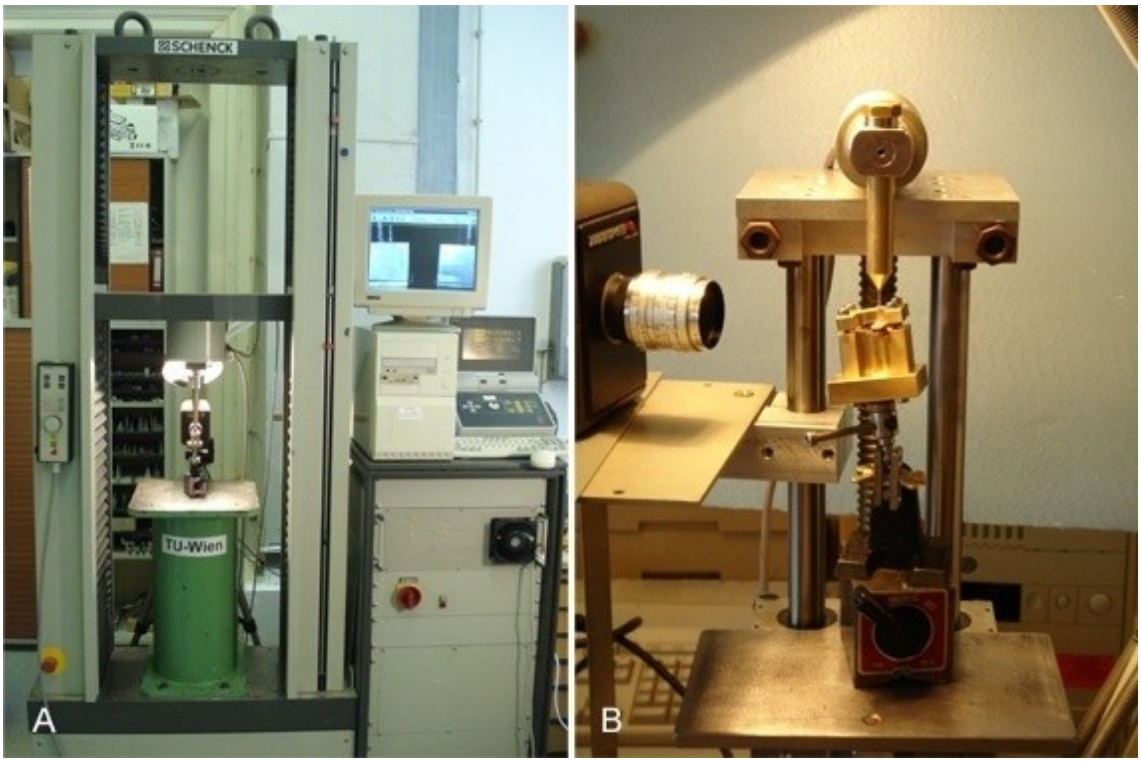

Figure 2-3. Mechanical test machines

(A) RSA100 (Carl Schenck AG), **(B)** Self-engineered mechanical testing device

Displacement was measured by a video extensometer system (camera: Philips Video40, Type LDH 0400/11, Philips Corporation, The Netherlands; software: "Punktvermessung für Windows", Version 1.1, Messphysik Materials Testing GmBH, Austria) (see Figure 2-3) in order to avoid a potential systematic error related to the rigidity of the test set up which does occur in displacement measurement by the crosshead of the materials testing machine (see also 2.2.6).

Furthermore a rigid test fixture (constructed by Gerald Holzlechner, Institute of Solid State Physics, Vienna University of Technology) was designed to allow for an accurate alignment of the samples as well as for a load transfer strictly perpendicular to the long axis of the implants (which could be achieved using 2 ball joints) (Figure 2-4 and Figure 2-10).

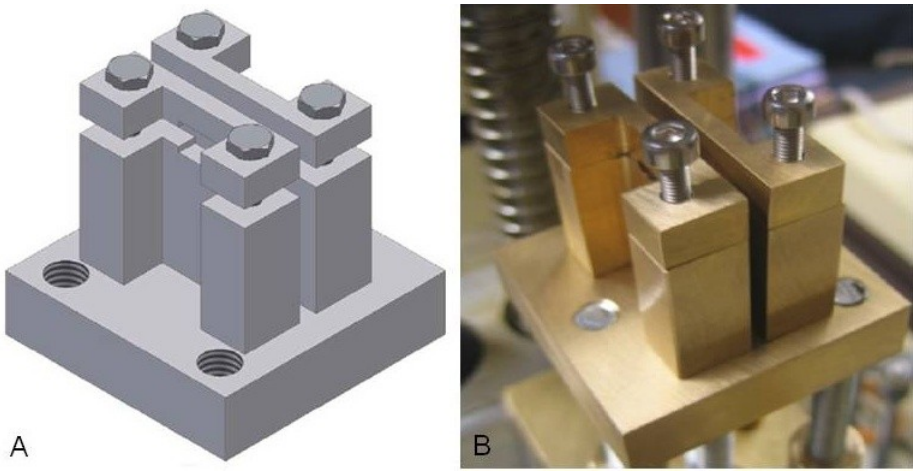

Figure 2-4. Test fixture

(A) CAD sketch and **(B)** photograph of our test fixture specially designed to ensure load transfer strictly perpendicular to the long axis of the implants. Femurs were mounted by tighting the four hexagon sockets (see also Figure 2-10).

This self-engineered test fixture was connected with an electromagnet via 2 ball joints. In turn, this electromagnet was used to affixed the construction to the level surface of the metal base (see also Figure 2-10).

2.1.7 Light Microscope

Olympus SZH ILLD binocular light microscope (Olympus Corporation) was used to examine mechanically tested samples microscopically. Digital images were captured using a DP20-5E digital microscope camera (Olympus Corporation)

2.1.8 Scanning Electron Microscope

Scanning electron microscopic examination was outsourced to the Department of Material Sciences and Process Engineering at the University of Natural Resources and Applied Life Sciences in vienna and performed by Prof. Stefanie Tschegg.

2.2 METHODS

2.2.1 Experimental Design

108 Sprague-Dawley rats five weeks of age were randomly assigned to 9 experimental groups (see Figure 2-5):

Rats of group 1, 2 and 3 received a new type of biodegradable implant made of a magnesium alloy (Mg implant) for 4, 12 and 24 weeks, respectively, whereas rodents of group 4, 5 and 6 received new PLGA pins (PLGA implant) for exactly the same evaluation periods. Rats of group 7, 8 and 9 implanted with standard titanium pins (titanium implant) for 4, 12 and 24 weeks, respectively, served as controls. Group 1, 2, 4, 5, 7 and 8 contained 13 rats each, whereas group 3, 6 and 9 included 10 rodents each.

Unthreaded uncoated smooth cylindrical pins with similar dimension (length: 7mm, diameter: 1,6 mm) and surface roughness but different modulus of elasticity were used in the present study.

The animals were allowed to acclimatise to laboratory conditions for one week prior to surgery. Pins were implanted bilaterally in the middiaphysis of the femoral bone with the same type of implant placed in both femora of each rat (→ 1 pin/femur, 2 pins/experimental animal and 1 implant type/experimental animal) (see also 2.2.2.2).

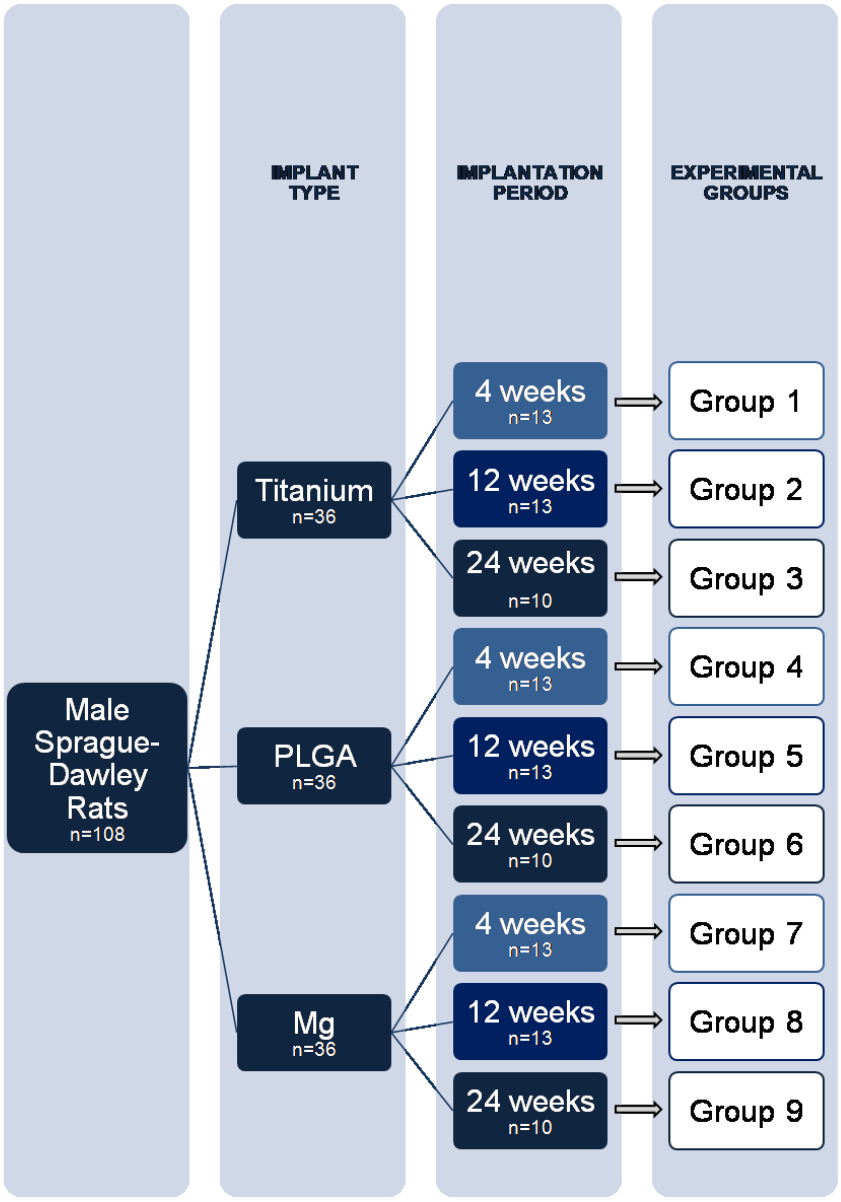

Figure 2-5. Schematic representation of experimental groups

All animals were subjected to the same experimental sequence (see Figure 2-6): Postoperatively, 4 different fluorochromes (Terramycin, Xylenolorange, Calcein and Calcein blue) were sequentially administered subcutaneously on day 14, 28, 56 and 84, respectively, in order to assess bone formation and remodeling at the bone-implant interface in vivo. The rodents were killed 4, 12 or 24 weeks after implantation according to experimental group; one harvested femur of each rat was allocated to the biomechanical testing group in a randomised manner whereas the contralateral femoral bone was embedded for further histomorphometric (data not

shown) and fluorescence microscopic analyses.

The retrieved bone-implant specimens assigned to the biomechanical testing group were immediately wrapped in saline-soaked gauze, sealed in airtight poly-ethylene tubes and storaged at -20°C. Subsequently three-dimensional bone-implant integration of these samples allocated to the biomechanical testing group was evaluated by means of micro-computed tomography. Thereafter a pushout test was performed so as to determine maximum pushout force, maximum shear strength, interface stiffness and energy absorption to failure in order to assess the biomechanical properties of the bone-implant interface. After mechanical testing, implant surfaces were qualitatively examined using a light microscope. Besides, two tested samples were exemplarily examined by means of scanning electron microscopy to clarify where the failure had occurred.

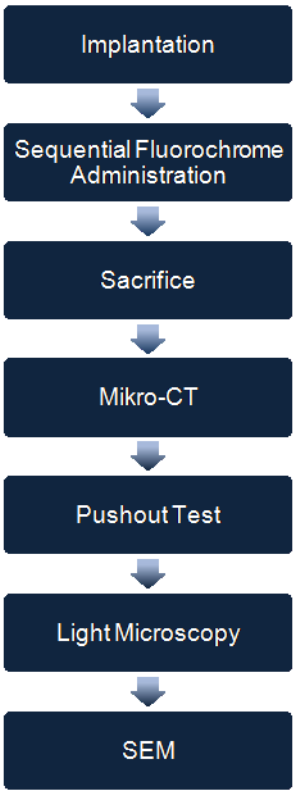

Figure 2-6: Flow chart of experimental design (see text for details)

2.2.2 Animal Experiments

The surgical procedure and euthanasia was performed at the special laboratories of the Center for Medical Research of the Medical University of Graz.

All animal experiments were approved by the Austrian Federal Ministry of Science and Research.

2.2.2.1 Anaesthesia

For surgery the animals were moved to the operating room. After weighing the rodents, general anesthesia was performed by an subcutaneous injection of Fentanyl® (Janssen-Cilag GmbH, Neuss, Germany) 20µg/kg body weight, Midazolam Delta® (Deltaselect GmbH, Dreieich, Germany) 400µg/kg body weight and Domitor® (Pfizer Corporation Austria GmbH, Vienna, Austria) 200µg/kg body weight.

2.2.2.2 Surgical Procedure

With the rats under general anesthesia, operating sites on both hind legs were shaved and sterilised using an iodine solution (Betaisodona®, Mundipharma GmbH, Limburg/Lahn, Germany). A skin incision (about 1,5 cm in length) was made at the lateral aspect of the posterior thigh with a scalpel (Figure 2-7, image A). The edges of the skin were retracted and fascia lata was transected longitudinally. The middiaphyseal region of femur was exposed through this lateral approach using scissors for blunt preparation (Figure 2-7, image B).

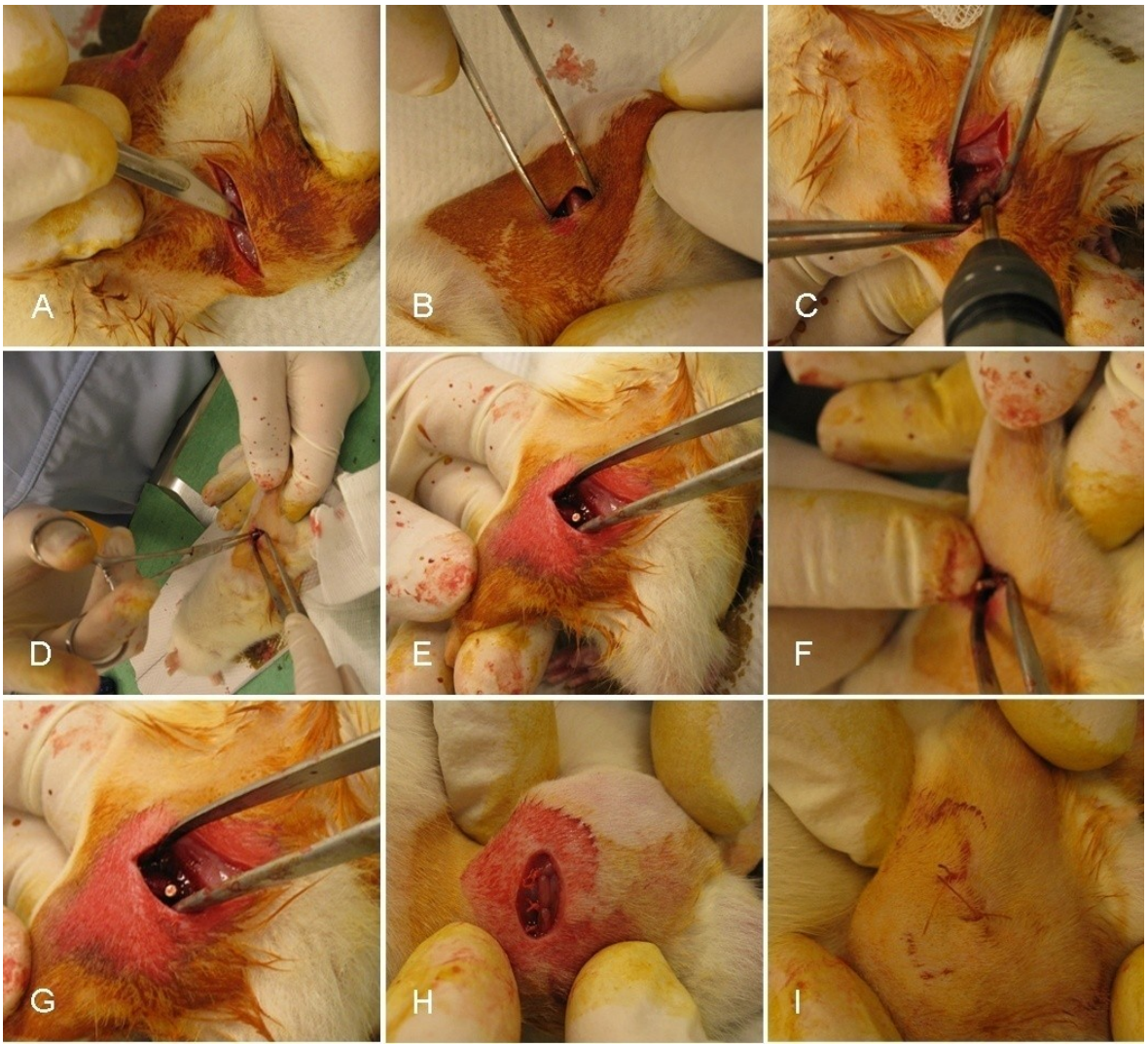

Figure 2-7. Surgical procedure (see text for details)

Thereafter a drill with ascending diameter was used to prepare the transcortical implantation bed in the middiaphysis of the femur (Figure 2-7, image C). The longitudinal axis of this drill hole was approximately perpendicular to the longitudinal axis of the femoral diaphysis. During the drilling profuse physiologic saline irrigation was applied via syringe in order to minimize frictional heat and thermal necrosis. Moreover drilling was performed at low rotational speed to this end. Now the cylindrical implant was inserted in the slightly undersized drill hole by gentle tapping resulting in press-fit fixation (Figure 2-7, image D and E). Transcortical placement was ensured by feeling for the medial pin end. (Figure 2-7, image F). We placed the implant centrally so that both ends protruded the cortical bone to

the same extent (Figure 2-7, image G). Subsequently the operating field was irrigated thoroughly with physiologic saline and iodine solution. In a final step the wound was closed in layers using absorbable Vicryle® 5.0 sutures (Ethicon, Norderstedt, Germany) (Figure 2-7, image H and I).

Contralateral implantation was performed in exactly the same way. Hence each rat received 2 implants (i.e., one pin was placed in the left, the other in the right mid-diaphyseal femur) made of the same material.

After completion of the surgical procedure the animals were tucked in and seated on a heating plate to avoid hypothermia. General anaesthesia was antagonized by an intraperitoneal injection of Narcanti® (Torrex Chiesi Pharma GmbH, Vienna, Austria) 120µg/kg body weigth, Anexate® (Roche Austria GmbH, Vienna, Austria) 50µg/kg body weigth and Antisedan® (Pfizer Corp. Austria GmbH, Vienna, Austria) 250µg/kg body weigth. After recovering from anesthesia the rodents were returned to their litters and were allowed immediate, unrestricted weight-bearing ad libitum. Daily clinical observation was performed throughout the implantation period.

2.2.2.3 Postoperative Pain Management

Postoperatively all of the animals were treated with Rimadyl® (Pfizer Corporation Austria GmbH, Vienna, Austria) 200mg/kg body weight which was daily subcutaneously injected for 1 week to ensure analgesia. From the eigth postoperative day forth Novalgin® drops (Sanofi-Aventis GmbH, Vienna, Austria) were added to the drinking water for another week (0,5ml Novalgin® per 400 ml drinking water) and Rimadyl was discontinued.

2.2.2.4 Euthanasia

According to experimental group rodents were killed 4, 12 or 24 weeks after implantation. For euthanasia the rats were carried to the operating room again and reweighed. Volatile Forane® (Abbot Laboratories Ltd., Kent, England) was administered for general anesthesia. Thereafter the heart was punctured and blood was aspirated for further examination (see 2.2.9). Subsequently 25mg Thiopental San-

doz® (Sandoz GmbH, Kundl, Austria) was injected into the cardiac ventricle in order to sacrifice the animal.

2.2.2.5 Preparation of Specimen

After sacrifice the Femora were harvested and cleaned of all soft tissue: A vast skin incision was made medially (Figure 2-8, image A), the capsules and ligaments of the hip and knee joint were dissected. Consequently the femur together with the surrounding muscle tissue could be carefully isolated by extraarticulation (Figure 2-8, image B-D). In a next step the circumjacent soft tissue was removed cautiously (Figure 2-8, image E-F). Any load transfer to the implanted pins was avoided during the whole procedure. After retrieval the cadavers were disposed according to the national law.

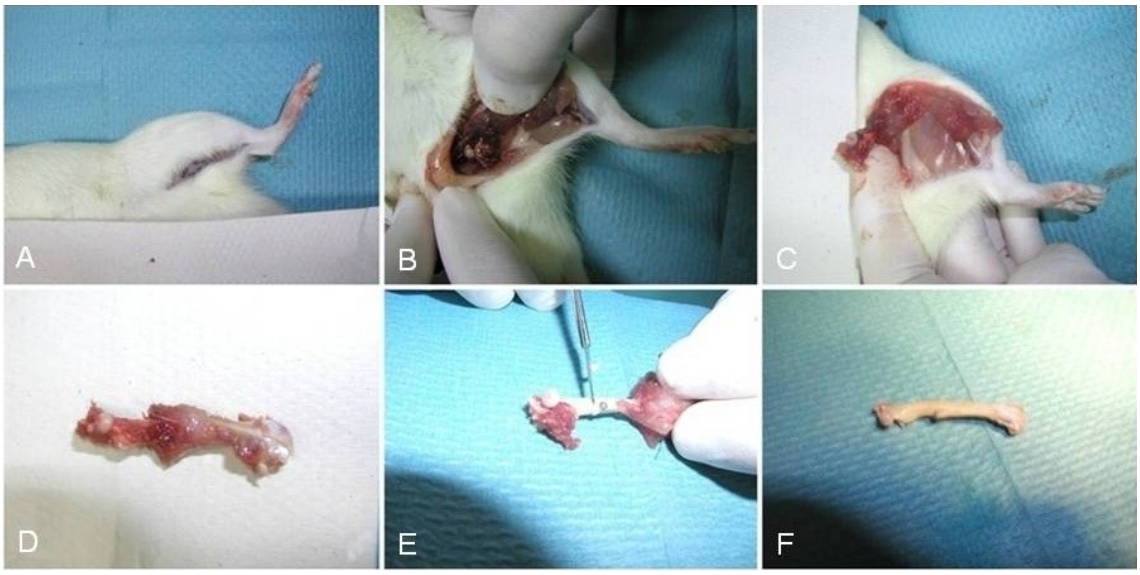

Figure 2-8 Retrieval and preparation of the femora (see text for details)

2.2.3 Fluorescent Labelling

We perfomed in vivo fluorescent labelling of bone using fluorochromes. Fluorochromes are calcium-binding substances which are deposited at the site of active mineralization. The resulting calcium-binding fluorescent dyes allow to asses bone formation and bone remodelling in vivo [81,82].

For this purpose we postoperatively administered 4 fluorochromes sequentially on day 14, 28, 56 and 84 by subcutaneous injection (Table 2-7).

Table 2-7: Details of applied fluorochromes including day of application and dosage based on bodyweight

Fluorochrome	Day	Dosage [mg/kg bodyweight]
Terramycin	14	40
Xylenolorange	28	90
Calcein	56	15
Calcein blue	84	30

After sacrifice 54 bone-implant specimens (6 per group) that were not tested bio-mechanically (see 2.2.1 Experimental Design) were dehydratet in a graded series of ethanol and embedded in Technovit 9100 New®:

Samples were fixed in 50% ethanol for 10 days. Thereafter, they were dehydrated with an ascending alcohol series (24h each) from 70%, 80%, 90%, 96%, 100% and 100% at 4°C in the fridge. Afterwards, the bones were defatted in xylenol and treated by Technovit 9100 New® solutions (1-4) as listed in Table 2-8.

Table 2-8. Technovit 9100 New(R) embedding (different solutions)

Name	Content	Duration
Sol. 1	60ml Xylenol + 60ml stabil. Basis solution	24 h at 4°C
Sol. 2	100ml stabil. Basis solution + 0.5g Catalysator 1	48 h at 4°C
Sol. 3	150ml destab. Basis solution[1] + 0.75g Catalysator 1	48 h at 4°C
Sol. 4[2]	150ml destab. Basis solution + 12g PMMA powder + 0.6g Catalysator 1	48 h at 4°C

Poly A[3]	360ml destab. Basis solution + 57.6g PMMA powder + 2.16g Catalysator 1	5 – 7 d at -20 C°
Poly B	40ml destab. Basis solution + 3.2ml Catalysator 2 + 1.6ml Regulator	5 – 7 d at -20 C°

[1] Destabilisation by mixing 1g $Al(OH)_3$ per 37.5 ml basis solution; [2] The solution is cloudy and has to be stirred over night at 4°C; [3] Polymerisators are mixed as follows: 9 parts poly A per 1 part poly B

After mixing poly A and poly B the bones were moved to special Teflon forms for embedding. The forms were covered with Technovit, sealed with a special foil and moved to a vacuum bag. After establishing a complete vacuum the polymerization took place at -20°C in the freezer (7-10 days).

After embedding the specimens were moved to the Bernhard Gottlieb University Vienna for further processing. After removing unnecessary embedding material stepwise grinding was used to generate ultra-thin sections of the specimens (this technique allows one section per bone; however the properties of the implant materials do not allow for conventional sectioning with microtomes).

Plastified blocks were processed with the Exakt Cutting and Grinding equipment (Exakt Apparatebau, Norderstedt, Germany). Ultrathin sections parallel to the long axis of the implants were prepared and stained with the Levai–Laczko dye.

These sections were subsequently analyzed using a fluorescence microscope in order to asses bone formation and active mineralization at the bone-implant interface over the implantation period in vivo.

2.2.4 Storage of Specimens

As above mentioned, one femur of each rat was randomly assigned to the biomechanical testing group. All these specimens were immediately wrapped in a gauze compress soaked with sterile 0.9% saline, sealed in airtight polyethylene tubes (as recommended by Johnson [54]) to prevent dehydration and storaged at -20°C. For µCT-scanning bone-implant specimens were wrapped in gauze soaked with sterile

saline and covered with a paraffin foil. After completion of the µCT-imaging samples were sealed in their abovementioned tubes again and were cryopreserved in the -20°C freezer until mechanical testing. For mechanical testing the frozen specimens were thawed for 3 hours at room temperature (wrapped in gauze soaked with physiologic saline and covered with plastic foil) and were kept moist throughout the test period using sterile physiologic saline. All bone-implant specimens were preserved (storage condition, packaging and thawing) in exactly the same manner. For the validity of the push-out test results it is of utmost importance that the mechanical properties of the tested cryopreserved bone-implant specimens correspond with the in vivo properties of freshly harvested specimens. In consideration of the up-to-date research data (see 1.3.5) we therefore chose this preservation modality because it does not significantly affect the biomechanical properties of our samples.

2.2.5 Microfocus Computed Tomography

The micro computer tomographic (µCT) measurements were performed with the VivaCT 75 (Scanco Medical, Bassersdorf, Switzerland). The scan resolution used was 20µm at an energy of 70 kV and a current of 114 µA. The integration time (the time one projection is measured) was 380ms, ensuring a very good picture quality. The number of slices varied from animal to animal because of the animal size. The evaluation was done from corticalis to corticalis resulting in about 90 – 120 slices per evaluation. For the subsequent analysis, two cylindric volumes of interest (VOIs) were selected as mentioned in Figure 2-9. The following morphological parameters were determined: bone volume per total tissue volume (BV/TV), mean trabecular thickness (Tb.Th) and bone-implant contact area (BIC).

A circle with a diameter 0.5mm bigger than the implants was chosen as the region of interest (ROI) for BV/TV-evaluation (see Figure 2-9, B). To avoid false positive measurements the circle was cut at the top and the bottom in order to exclude the cortical bone.

For the assessment of the bone-implant contact area (BIC), the samples were automatically segmented with different implant thresholds (titanium: 700, Mg: 550,

PLGA: 1000) due to different material densities and x-ray absorption. The region of interest (ROI) for bone-implant contact area (BIC) evaluation was defined as a 3 pixel thick ring, 2 pixels away from the implant (see Figure 2-9, A).

µCT Measurement V6.0 was used for scanning. The µCT Evaluation V6.0 and the image processing language V5.06b were used for sample evaluation. This software package is the built-in software delivered with the VivaCT75.

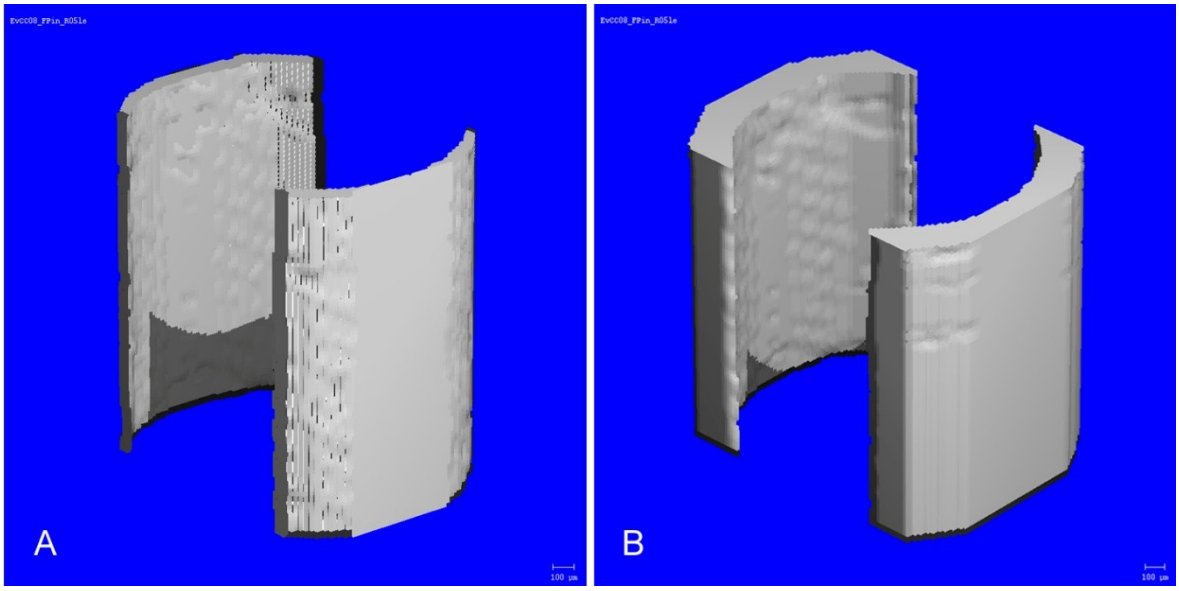

Figure 2-9. Volumes of interest (VOIs) for determination of (A) BIC and (B) BV/TV as well as Tb.Th

2.2.6 Pushout Test

2.2.6.1 Biomechanical Test Setup

A self-engineered mechanical testing device (see 2.1.6) was used for pushout testing of bone-implant specimens retrieved after an implantation period of 4 weeks (group 1, 4 and 7). Samples harvested after an evaluation period of 12 as well as 24 weeks (group 2, 3, 5, 6, 8 and 9) were mechanically tested with use of a testing machine with higher performance (RSA100, Carl Schenck AG, Darmstadt, Germany) because pushout tests of specimens implanted for 4 weeks yielded unexpected high maximum pushout forces for Mg implants. The same plunger, push

rod, test fixture and video extensometer system were used in both cases. The biomechanical test setup was developed with regard to the up-to-date scientific literature addressing important test conditions of pushout tests (interface stress distribution, clearance of the hole in the support jig, accurate alignment, displacement measurement, displacement rate etc.). The detailed theoretical background is mentioned above (see 1.3.3.1). Displacement was measured by means of a video extensometer in order to avoid a potential systematic error related to the rigidity of the test set up which does occur in displacement measurement by the crosshead of the materials testing machine. Since implant loading strictly perpendicular to the long axis of the pin is crucial in pushout testing a specific test fixture specially designed for this purpose (see also 2.1.6) was utilised to allow for an accurate alignment of the samples as well as for a strictly perpendicular axial load transfer.

Samples were thawed for 3 hours at room temperature wrapped in gauze soaked with sterile 0.9% saline and covered with plastic foil to prevent dehydration. Throughout the testing procedure, the specimens were kept moist by frequent application of physiologic saline solution. Then each bone-implant specimen was mounted on the test fixture and thoroughly orientated so that the line of action of the loading force was collinear with the long axis of the pin (see Figure 2-10). Furthermore accurate alignment among the push rod, the specimen and the test fixture was ensured. The diameter of the push rod was 1mm, the clearance of the brackets of the test fixture which supported the bone was 4.5 mm (see Figure 2-10). Each specimen was loaded at a constant displacement rate of 1.8 mm/min and all samples were tested to failure. Simultaneous recordings were made of displacement, as measured by the video extensometer, and of the load, as recorded from the load cell transducer. Analysed biomechanical parameters were determined from recorded load-displacement curves using ORIGIN PRO 7.5 software package (OriginLab Corporation, Northampton, USA).

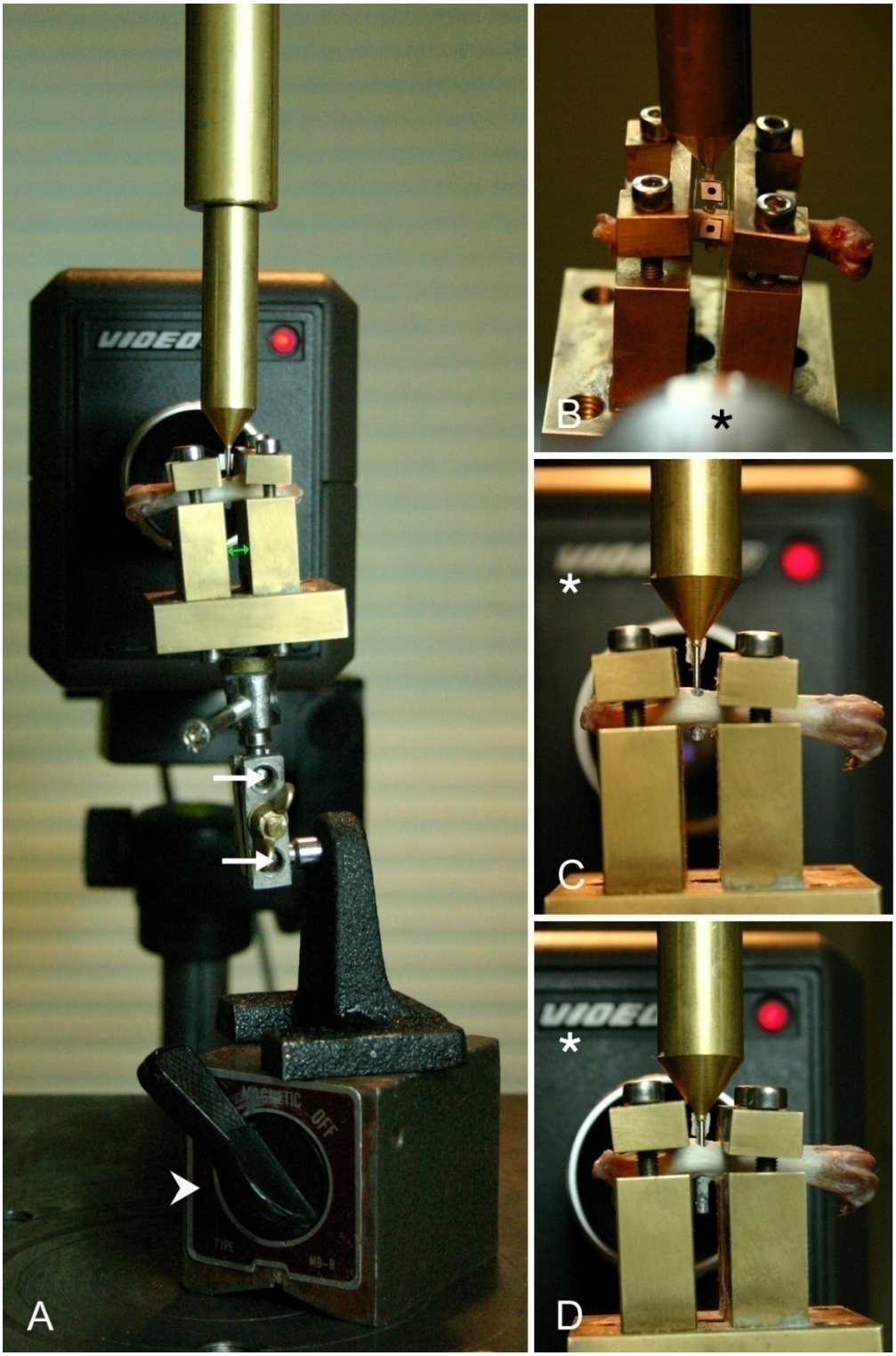

Figure 2-10. Experimental set up

(A) Specimens were mounted on the test fixture by tighting the four hexagon sockets (clearance oft the brackets supporting the bone: 4.5 mm *(green double arrow)*). 2 ball joints *(arrows)* allowed for a load transfer strictly perpendicular to the long axis of the implant. This rigid construction was affixed to a metal base by an electromagnet *(arrowhead)*.**(B)** Displacement was recorded with use of a video extensometer *(asterisks)* measuring the distance between two black dots. **(C)** It was ensured that the line of action of the loading force was collinear with the long axis of the pin. **(D)** Tested sample after pushout test.

2.2.6.2 Determined Biomechanical Parameters

The following well established biomechanical parameters were determined by means of a pushout test in order to assess and compare the interfacial biomechanical properties of the different implant types tested in the present study:

2.2.6.2.1 Maximum Pushout Force (F_{max})

Maximum pushout force (F_{max}) [N] (also referred to as “peak force” or “ultimate load” or “interface shear modulus”) was determined as maximum load at the beginning of implant displacement (typically followed by a load decline) for titanium implants and nBM-implants. Load displacement curves of these implant types showed typical and very similar curve progressions. However, curve progressions of tested PLGA implants showed considerably differing characteristics (see also `Discussion´). Hence F_{max} was considered as the maximum force recorded during mechanical testing regardless of implant displacement for the sake of clarity as well as reproducibility.

2.2.6.2.2 Ultimate Shear Strength (σ_u)

Ultimate shear strength of the interface (σ_u) [N/mm^2] (also referred to as “maximum shear stress” or “ultimate shear stress”) was calculated by dividing the maximum pushout force by the bone-implant contact area measured with use of a calliper gauge (BIC_{Cg}):

$$\boldsymbol{\sigma_u = F_{max}/}\ BIC_{Cg}\ [N/mm^2]$$

F_{max}: maximum axial pushout force

$BIC_{Cg} = \pi DL$ (see also 2.2.10)

D: outer diameter of the cylindrical implant

L: mean length of bone in contact with the implant measured by means of a calliper gauge

2.2.6.2.3 Interface Stiffness

Interface stiffness [N/mm] (also referred to as “apparent shear stiffness”, “apparent shear modulus” or “interface shear modulus”) was measured as the slope of the load-displacement curve in its linear region.

2.2.6.2.4 Energy Absorption To Failure

Energy absorption to failure [Nmm=mJ] was calculated as the area under the load-displacement curve until failure (i.e., maximum pushout force).

2.2.7 Light Microscopy

Mechanically tested bone-implant samples were examined microscopically: Standardised digital images were taken from anterior and posterior; pin degradation of bioarbsorbable implants and implant surface was qualitatively analysed.

2.2.8 Scanning Electron Microscopy

Two biodegradable implants (1 PLGA implant and 1 Mg implant) were examined by means of scanning electron microscopy to clarify where the failure had occurred (within the trabecular bone or at the bone-implant interface).

2.2.9 Blood Examination

In order to discover potential systemic inflammatory reactions as a result of pin implantation (due to a potential lack of biocompatibility of the investigated biodegradable implants) we performed blood smears from each animal:

Blood was aspirated from the cardiac ventricle of each anaesthetised rat prior to sacrifice by injection of an overdose thiopental. A 2-3 mm drop of blood was placed on the slide and spread using a second slide (spreader slide). The slides were air dried and stained with Pappenheim (May-Grünwald-Giemsa). Subsequently the smears were examined microscopically: 100 cells were counted and sorted by cell type. The cellular distribution of lobulated neutrophil granulocytes, stab neutrophils, eosinophil granulocytes, basophil granulocytes, monocytes and

lymphocytes was assessed resulting in the percentage of each cell type (relative differential count).

2.2.10 Determination of Bone-Implant Contact Area

Bone-implant contact area was determined with use of a calliper gauge (BIC_{Cg}) and was subsequently used to calculate ultimate shear strength (see 2.2.6.2.2).

BIC_{Cg} was assessed by calliper gauge as follows: The length of bone in contact with the implant was measured at 4 well-defined sites (cranial, caudal, anterior and posterior) for each specimen by two independent observers prior to mechanical testing in a standardised manner (see Figure 2-11).

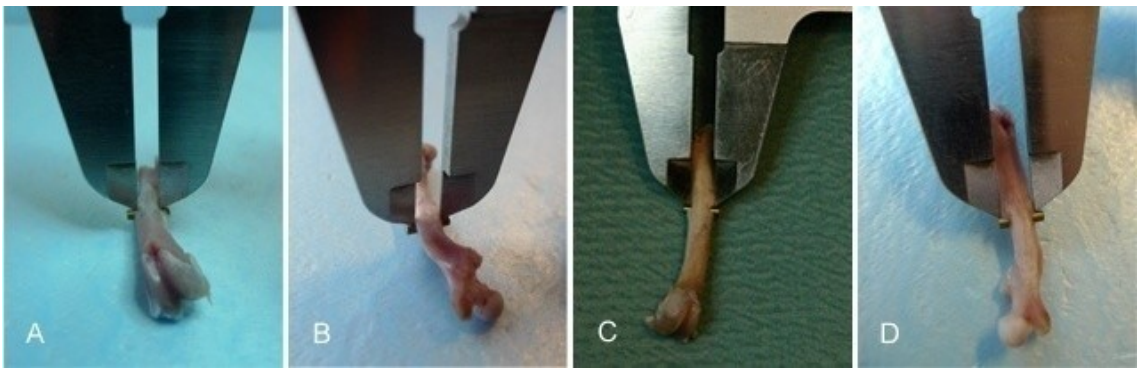

Figure 2-11. Determination of bone-implant contact area by calliper gauge

Length of bone in contact with the implant was measured at 4 well-defined sites **(A)** anteriorly, **(B)** posteriorly, **(C)** proximally and **(D)** distally to the pin in a standardised manner. In the first instance averaged interface length and finally BICcg was calculated (see text for details).

The average interface length was calculated from the 4 distances measured by each observer and used to determine bone-implant contact area (BIC = π*implant diameter*average interface length). Finally the resulting BIC-values of both observers were averaged to obtain the mean bone-implant contact area measured by calliper gauge (BIC_{cg}).

2.2.11 Statistical Analysis

Microsoft Excel® (Microsoft Corporation, Redmond, WA, USA) was used for data administration. All statistical evaluations and data presentation were performed with SPSS 16.0® (SPSS Inc., Chicago, IL, USA).

Demographic data of the different parameters was displayed as mean and standard deviation in case of normal distribution or rather as median and first as well as third quartile if data was non-normally distributed.

Normality of data was checked by Kolmogorov-Smirnov test.

For normally distributed data, one-way ANOVA was applied. If Levene's test of homogeneity of variance was not significant, one-way ANOVA and Scheffe post hoc tests were performed to attain all possible pairwise comparisons. In case of heterogeneous variances Welch one-way ANOVA was used followed by Tamhane´s T2 post hoc tests.

For data lacking normal distribution, first Kruskal-Wallis-Tests were performed to search for significant global differences. In case of global differences pairwise analysis was done by Mann-Whitney U tests. Due to multiple testing p-values had to be adjusted by Bonferroni correction to avoid accumulation of α-mistakes.

P-values of less than 0.05 were considered as statistically significant.

3 RESULTS

Six of 108 rodents were lost intraoperatively due to anaesthetic complications or femoral fracture in consequence of drilling. All other animals tolerated the operation well and regained full weight-bearing. Healing occurred uneventfully and no signs of inflammation, gross infection or tissue reaction could be observed throughout the implantation period.

Kolmogorov-Smirnov testing revealed normality of distribution for bone volume (BV/TV), bone-implant contact area (BIC), trabecular thickness (Tb.Th.), lobulated neutrophils, monocytes and lymphocytes, whereas data of maximum pushout force, ultimate shear strength, energy absorption to failure, interface stiffness, stab neutrophils, eosinophil neutrophils and basophil neutrophils were not normally distributed.

3.1 PUSHOUT TEST

Technical problems precluded data analysis of 11 bone-implant specimens (3 specimen fractured when mounted on the test fixture, 4 tilted over during testing and in 4 samples recording load-displacement curve failed) so that 91 samples were successfully tested ultimately (Table 3-1).

Table 3-1. Number of samples successfully tested in pushout test

Implantation period	**Implant type**			
	Tn [n=]	Mg-alloy [n=]	nPLGA [n=]	
1 month	13	12	11	36
3 months	7	12	11	30
6 months	9	8	8	25
	29	32	30	**91**

The resulting load-displacement curves were analysed and maximum pushout

force, ultimate shear strength, energy absorption to failure and interface stiffness were determined. The obtained data is summarised in Table 3-2, pushout force as well as ultimate shear strength are additionally represented as box plots in Figure 3-1. Interface stiffness (measured as the slope of the load-displacement curve in its linear region) could not be assessed for PLGA implants after 1 and 3 months in consequence of their typical load-displacement curve progression lacking linear regions (see also `Discussion´).

Table 3-2. Maximum pushout force (F_{max}), ultimate shear strength (σ_u), energy absorption to failure (EA) and interface stiffness (Stiffness) for each implantation period and implant type (median, first and third quartile (in parentheses))

IP	IT	F_{max} [N]	σ_u [N/mm^2]	EA [mJ]	Stiffness [N/mm]
1 m	Tn	23.58 (11.55 – 30.99)	1.12 (0.57 – 1.50)	0.39 (0.17 – 0.79)	1161.76 (698.09 – 1424.96)
	Mg	49.35 (37.63 – 55.53)	2.43 (1.80 – 2.81)	1.07 (0.92 – 1.40)	1423.49 (1116.70 – 2761.96)
	PLGA	15.65 (12.31 – 35.13)	0.69 (0.54 – 1.66)	17.18 (8.68 – 44.35)	NM
3 m	Tn	100.83 (80.10 – 109.59)	4.14 (3.25 – 4.55)	3.24 (2.23 – 7.41)	1466.34 (1380.49 – 2292.41)
	Mg	151.87 (133.30 – 185.33)	6.19 (5.29 – 7.23)	12.45 (9.08 – 18.70)	1965.52 (1712.93 – 3817.18)
	PLGA	45.71 (31.22 – 57.71)	1.83 (1.20 – 2.56)	59.79 (41.92 – 71.25)	NM
6 m	Tn	44.78 (30.57 – 90.10)	2.14 (1.26 – 3.53)	0.70 (0.36 – 1.46)	1849.04 (1593.73 – 3641.10)
	Mg	185.16 (157.73 – 221.98)	7.65 (6.61 – 8.71)	22.64 (11.05 – 36.86)	2067.43 (1490.42 – 2511.55)
	PLGA	42.79 (29.69 – 55.01)	1.67 (1.11 – 2.09)	18.40 (10.89 – 25.22)	274.64 (208.20 – 397.21)

IP = implantation period; m = month(s); IT = implant type; NM = could not be measured due to irregular load-displacement curve progression lacking linear regions

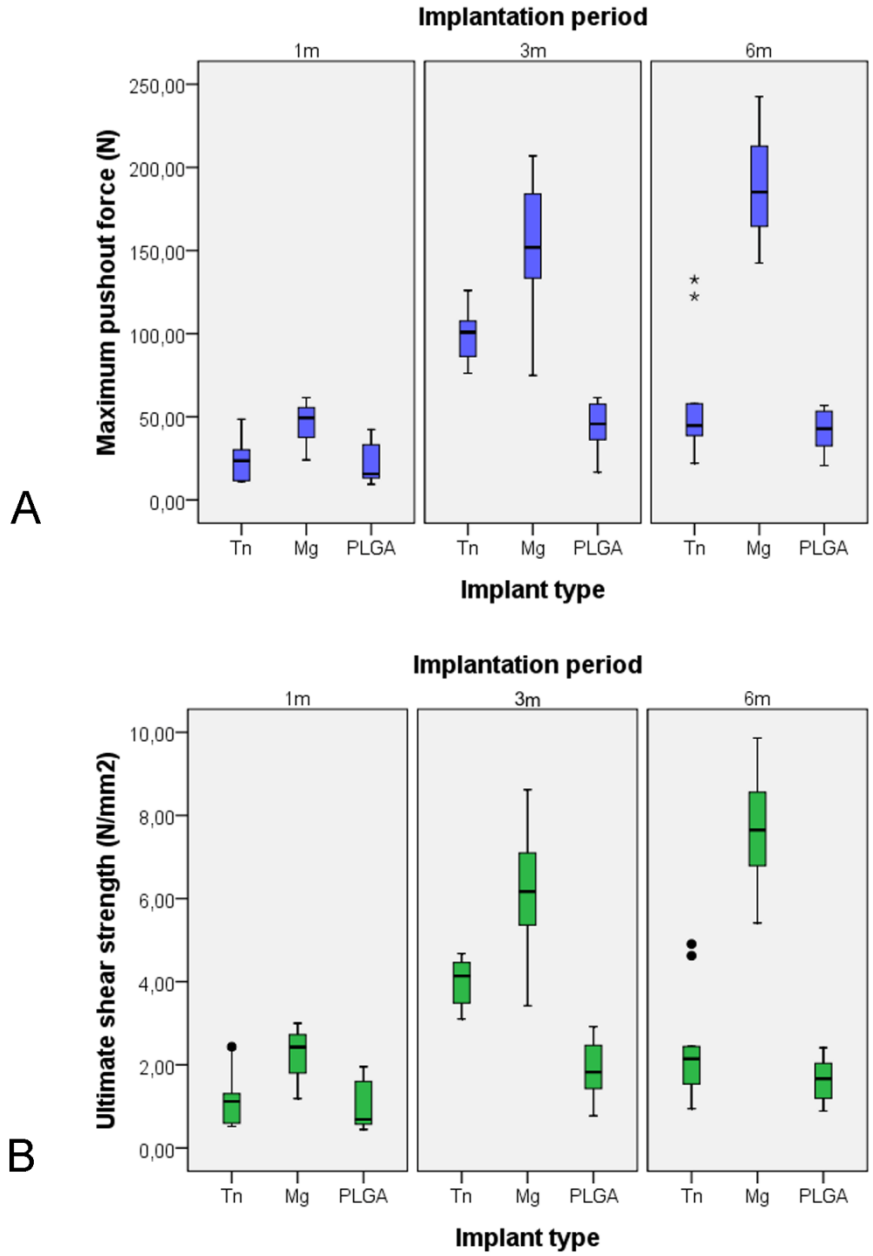

Figure 3-1. Maximum pushout force (A) and ultimate shear strength (B) for each implant type and implantation period represented by box plots

The lines within the boxes indicate the median (50th percentile), the upper and lower ends of the boxes indicate the first quartile (25th percentile) and the third quartile (75th percentile), respectively.

Kruskal-Wallis-Tests were performed for each implantation period to search for significant global differences among different implant types (Table 3-3).

Table 3-3. Global differences in biomechanical parameters among different implant types within each implantation period using Kruskal-Wallis-Tests

Implantation period	F_{max} [N]	σ_u [N/mm^2]	EA [mJ]	Stiffness [N/mm]
1 month	0.001**	0.001**	< 0.001**	0.057‡
3 months	< 0.001**	< 0.001**	< 0.001**	0.128‡
6 months	< 0.001**	< 0.001**	0.001**	< 0.001**

* $p < 0.05$, ** $p < 0.01$; ‡ Interface stiffness could not be measured for PLGA implants after 1 and 3 months, thus only Tn and Mg were compared after these implantation periods; F_{max} = maximum pushout force, σ_u = ultimate shear strength, EA = energy absorption to failure, Stiffness = interface stiffness.

In case of significant global differences pairwise comparisons between different implant types were performed using Mann-Whitney U tests with Bonferroni corrections (Table 3-4):

These pairwise analyses yielded highly significantly greater **maximum push out forces** as well as **ultimate shear strengths** in Mg implants than in Tn and PLGA pins after each implantation period, whereas median maximum pushout force values of Mg implants were up to 4 fold higher compared to the other pins. Tn and PLGA did not differ significantly except for an implantation period of 3 months.

Energy absorption to failure (EA) was found to be significantly greater in PLGA than in Mg pins except for an implantation period of 6 months, in turn EA values of Mg implants were higher than those of Tn pins.

Interface stiffness was similar in Tn and Mg implants, but considerable lower in PLGA pins after 6 months.

Table 3-4. Pair-wise analysis of global differences in biomechanical parameters among different implant types within each implantation period by Mann-Whitney-U-Tests with Bonferroni corrections

Implantation Period	Analysed pairs	F_{max} [N]	σ_u [N/mm^2]	EA [mJ]	Stiffness [N/mm]
1 month	Tn vs. Mg	< 0.001**	0.003**	0.009**	NSGD
	Tn vs. PLGA	1	1	< 0.001**	NA
	Mg vs. PLGA	0.003**	< 0.001**	< 0.001**	NA
3 months	Tn vs. Mg	0.006**	0.003**	0.003**	NSGD
	Tn vs. PLGA	< 0.001**	< 0.001**	< 0.001**	NA
	Mg vs. PLGA	< 0.001**	< 0.001**	< 0.001**	NA
6 months	Tn vs. Mg	< 0.001**	< 0.001**	0.006**	1
	Tn vs. PLGA	1	1	< 0.001**	< 0.001**
	Mg vs. PLGA	< 0.001**	< 0.001**	1	< 0.001**

* $p < 0.05$, ** $p < 0.01$; NSGD = No significant global differences in the previous Kruskal-Wallis test; NA = could not be analysed because interface stiffness was not measured for PLGA after 1 as well as 3 months; F_{max} = maximum pushout force, σ_u = ultimate shear strength, EA = energy absorption to failure, Stiffness = interface stiffness.

Moreover, we analysed if there are any statistically significant differences in biomechanical parameters between the three implantation periods within each type of implant. In other words, we searched for time-dependant changes of maximum pushout force, ultimate shear strength, energy absorption to failure and interface stiffness within each implant type. As before, Kruskal-Wallis tests (Table 3-5) and subsequent Mann-Whitney-U-Tests with Bonferroni corrections (Table 3-6) were applied:

Table 3-5. Global differences in biomechanical parameters among different implantation periods within each implant type using Kruskal-Wallis-Tests

Implant type	F_{max} [N]	σ_u [N/mm^2]	EA [mJ]	Stiffness [N/mm]
Tn	< 0.001**	< 0.001**	0.014*	0.002**
Mg	< 0.001**	< 0.001**	< 0.001**	0.192

PLGA	0.005**	0.020*	0.003**	NM

* p < 0.05, ** p < 0.01; NA = could not be analysed because interface stiffness was not measured for PLGA after 1 as well as 3 months; F_{max} = maximum pushout force, σ_u = ultimate shear strength, EA = energy absorption to failure, Stiffness = interface stiffness.

Maximum pushout force, ultimate shear strength as well as energy absorption to failure were found to be significantly greater in all three implant types after an implantation duration of 3 months compared to 1 month (Figure 3-2). For example, median maximum pushout force values of Tn, Mg and PLGA pins were about 4.3, 3.1 and 2.9-fold higher, respectively. Between 3 and 6 months of implantation, no significant differences in biomechanical parameters were detected in any of the investigated implants except for EA of PLGA pins which significantly decreased.

Table 3-6. Pair-wise analysis of global differences in biomechanical parameters among different implantation periods within each implant type by Mann-Whitney-U-Tests with Bonferroni corrections

Implant type	Analysed pairs	F_{max} [N]	σ_u [N/mm^2]	EA [mJ]	Stiffness [N/mm]
Tn	1 mo vs. 3 mo	< 0.001**	< 0.001**	0.024*	0.072
	1 mo vs. 6 mo	0.018*	0.051	0.432	< 0.001**
	3 mo vs. 6 mo	0.165	0.165	0.126	0.897
Mg	1 mo vs. 3 mo	< 0.001**	< 0.001**	< 0.001**	NSGD
	1 mo vs. 6 mo	< 0.001**	< 0.001**	0.009**	NSGD
	3 mo vs. 6 mo	0.141	0.171	0.405	NSGD
PLGA	1 mo vs. 3 mo	0.006**	0.024*	0.015*	NA
	1 mo vs. 6 mo	0.036*	0.153	1	NA
	3 mo vs. 6 mo	1	1	0.003**	NA

* p < 0.05, ** p < 0.01; NSGD = No significant global differences in the previous Kruskal-Wallis test; NA = could not be analysed because interface stiffness was not measured for PLGA after 1 as well as 3 months; F_{max} = maximum pushout force, σ_u = ultimate shear strength, EA = energy absorption to failure, Stiffness = interface stiffness.

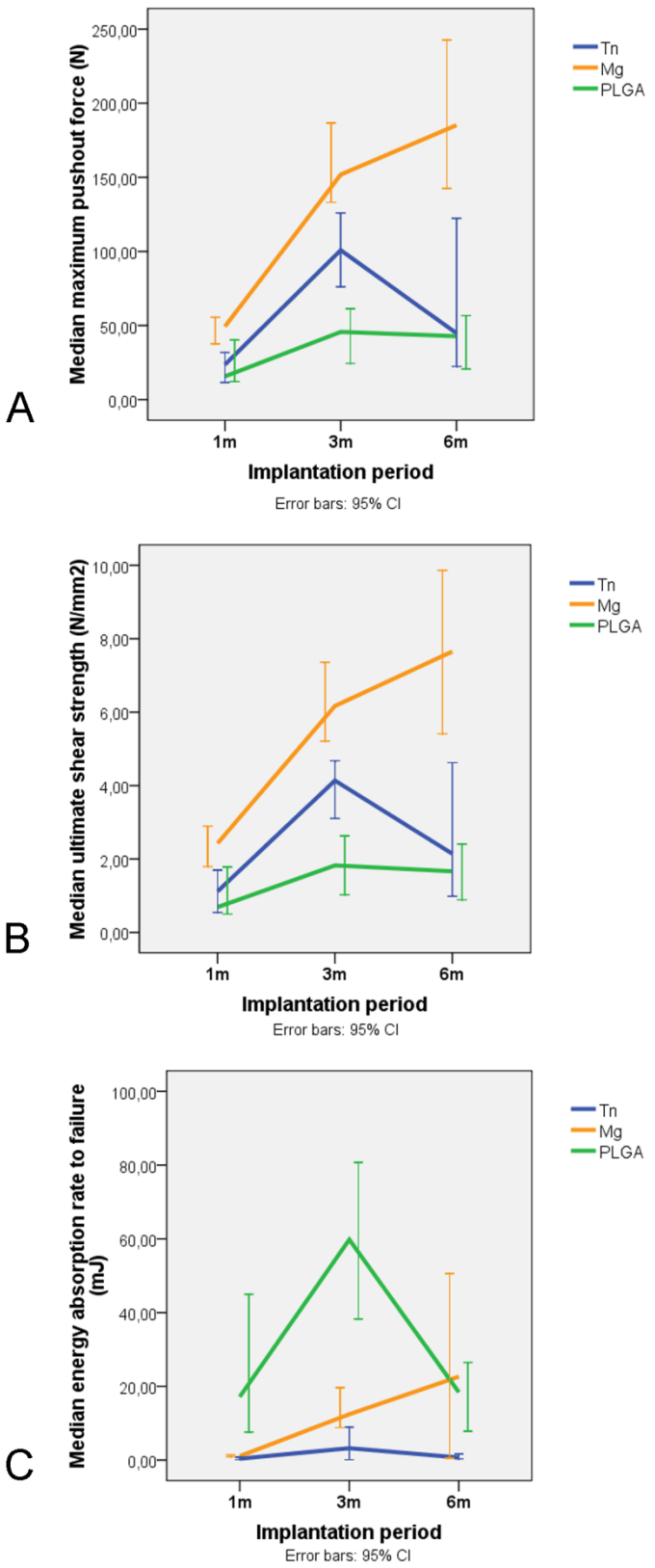

Figure 3-2. Median (A) maximum pushout force, (B) ultimate shear strength and (C) energy absorption to failure after 1, 3 and 6 months of implantation

3.2 MICROFOCUS COMPUTED TOMOGRAPHY

All harvested bone-implant specimens of each group (n = 102) were examined by means of microfocus computed tomography. Three-dimensional images were reconstructed for a few samples (Figure 3-3).

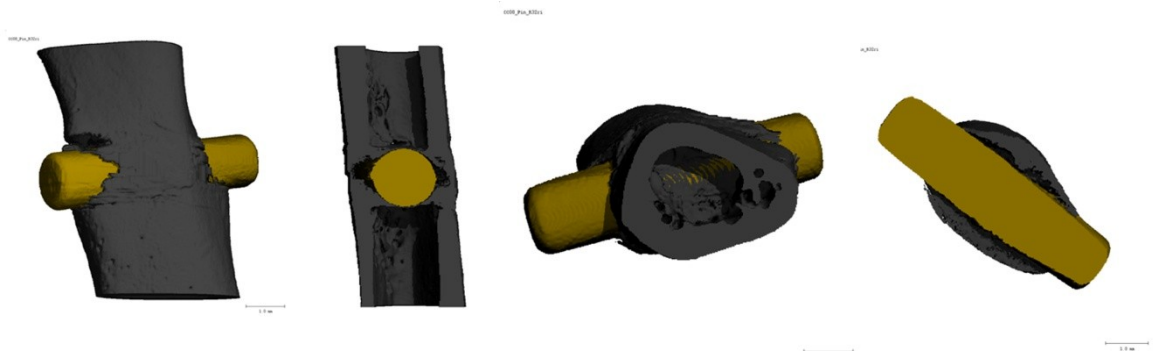

Figure 3-3. Three-dimensional reconstruction of a bone-implant specimen retrieved 4 weeks after implantation (titanium pin)

Furthermore, bone volume per tissue volume (BV/TV), mean trabecular thickness (Tb.Th) and bone-implant contact area (BIC) were quantitatively assessed for each specimen. The obtained data is summarised in Figure 3-7 and also represented as error bars in Figure 3-4.

Table 3-7. MicroCT data for each implantation period and implant type (mean ± standard deviation (SD))

Implantation period	Implant type	n	BV/TV‡	Tb.Th [Voxel]	BIC‡
1 month	Tn	14	0.16 ± 0.06	0.11 ± 0.02	0.27 ± 0.01
	Mg	12	0.24 ± 0.10	0.13 ± 0.02	0.42 ± 0.13
	PLGA	12	0.18 ± 0.07	0.14 ± 0.01	0.18 ± 0.08
3 months	Tn	9	0.22 ± 0.07	0.13 ± 0.01	0.37 ± 0.09
	Mg	13	0.33 ± 0.10	0.15 ± 0.02	0.53 ± 0.13
	PLGA	12	0.35 ± 0.12	0.14 ± 0.02	0.50 ± 0.19

6 months	Tn	10	0.21 ± 0.09	0.13 ± 0.01	0.33 ± 0.11
	Mg	10	0.37 ± 0.16	0.14 ± 0.03	0.66 ± 0.19
	PLGA	10	0.33 ± 0.10	0.13 ± 0.01	0.54 ± 0.14

n = number of scanned samples; BV/TV = bone volume/tissue volume; Tb.Th. = mean trabecular thickness; BIC = bone-implant contact area; ‡ BV/TV and BIC are given as percentages converted to decimal fractions.

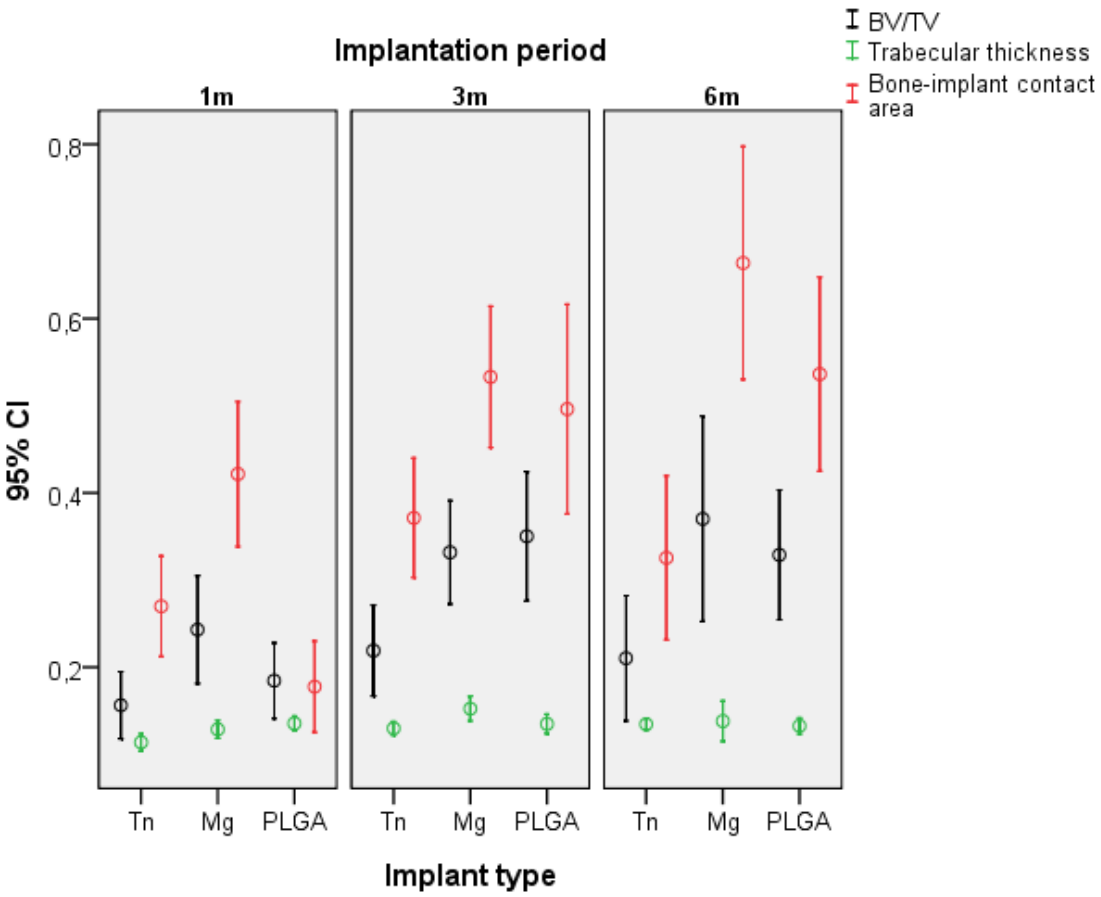

Figure 3-4. Error bars representing means and confidence intervals for means of microCT data for each implant type and implantation period

One-way ANOVA was conducted to test for differences among the different implant types within each implantation period (Table 3-8).

Table 3-8. Differences in microCT parameters among different implant types within each implantation period using one-way ANOVA

Implantation period	BV/TV	Tb.Th	BIC
1 month	0.027*	0.004**	< 0.001**
3 months	0.012*	0.017*	0.048*
6 months	0.020*	0.862	< 0.001**

* p < 0.05, ** p < 0.01; BV/TV = bone volume/tissue volume; Tb.Th. = mean trabecular thickness; BIC = bone-implant contact area;

Significant differences were then further analysed by pairwise comparisons between different implant types using Scheffe and Tamhane´s T2 Post hoc tests (

Table 3-9):

Bone-implant contact area was significantly higher in **Mg implants** than in titanium implants after 1 and 6 months of implantation and than in PLGA implants after 1 month. Moreover, Mg implants showed significantly higher BV/TV after 1 and 3 months and higher trabecular thickness (Tb.Th) after 3 months compared to titanium implants.

Furthermore, it was found that BIC after 6 months, BV/TV after 3 months and mean trabecular thickness after 1 month were significantly higher in **PLGA implants** than in titanium pins.

Table 3-9. Pairwise analysis of differences in microCT parameters among different implant types within each implantation period by one-way ANOVA Post Hoc Tests[1]

Implantation-Period	Analysed pairs	BV/TV	Tb.Th	BIC
1 month	Tn vs. Mg	0.030*	0.064	0.004**
	Tn vs. PLGA	0.665	0.005**	0.103
	Mg vs. PLGA	0.195	0.559	< 0.001**
3 months	Tn vs. Mg	0.043*	0.030*	0.055
	Tn vs. PLGA	0.018*	0.825	0.175

	Mg vs. PLGA	0.897	0.079	0.823
6 months	Tn vs. Mg	0.055	NSGD	< 0.001**
	Tn vs. PLGA	0.051	NSGD	0.032*
	Mg vs. PLGA	0.883	NSGD	0.219

[1] Scheffe post hoc tests were performed in case of homogeneous variances, Tamhane´s T2 post hoc tests were used if variances were heterogeneous; NSGD = No significant differences in the previous one-way ANOVA; * $p < 0.05$, ** $p < 0.01$; BV/TV = bone volume/tissue volume; Tb.Th. = mean trabecular thickness; BIC = bone-implant contact area.

Furthermore, one-way ANOVA (Table 3-10) and subsequent Post hoc tests (Table 3-11) were utilised to assess time-dependent changes (i.e., differences among the 3 implantation periods) in these parameters within each implant type:

Table 3-10. Differences in microCT parameters among different implantation periods within each implant type using one-way ANOVA

Implant type	BV/TV	Tb.Th	BIC
Tn	0.099	0.002**	0.073
Mg	0.050	0.060	0.003**
PLGA	< 0.001**	0.906	< 0.001**

* $p < 0.05$, ** $p < 0.01$; BV/TV = bone volume/tissue volume; Tb.Th. = mean trabecular thickness; BIC = bone-implant contact area.

Between 1 and 3 months of implantation, **BV/TV** as well as **bone-implant contact area** significantly increased in PLGA implants (Figure 3-5). In addition, **trabecular thickness** was significantly greater in titanium implants after an implantation period of 3 months compared to 1 month. In Mg implants, a significant increase of bone-implant contact area between 1 and 6 months was found (Figure 3-5). Furthermore, no significant differences in microCT parameters were detected in any of the investigated implants between 3 and 6 months of implantation (see Table 3-11).

Table 3-11. Pairwise analysis of differences in microCT parameters among different implantation periods within each implant type by one-way ANOVA Post Hoc Tests[1]

Implant type	Analysed pairs	BV/TV	Tb.Th	BIC
Tn	1 mo vs. 3 mo	NSGD	0.025*	NSGD
	1 mo vs. 6 mo	NSGD	0.005**	NSGD
	3 mo vs. 6 mo	NSGD	0.748	NSGD
Mg	1 mo vs. 3 mo	NSGD	NSGD	0.194
	1 mo vs. 6 mo	NSGD	NSGD	0.003**
	3 mo vs. 6 mo	NSGD	NSGD	0.133
PLGA	1 mo vs. 3 mo	0.001**	NSGD	< 0.001**
	1 mo vs. 6 mo	0.007**	NSGD	< 0.001**
	3 mo vs. 6 mo	0.881	NSGD	0.930

[1] Scheffe post hoc tests were performed in case of homogeneous variances, Tamhane´s T2 post hoc tests were used if variances were heterogeneous; NSGD = No significant differences in the previous one-way ANOVA; * $p < 0.05$, ** $p < 0.01$; BV/TV = bone volume/tissue volume; Tb.Th. = mean trabecular thickness; BIC = bone-implant contact area.

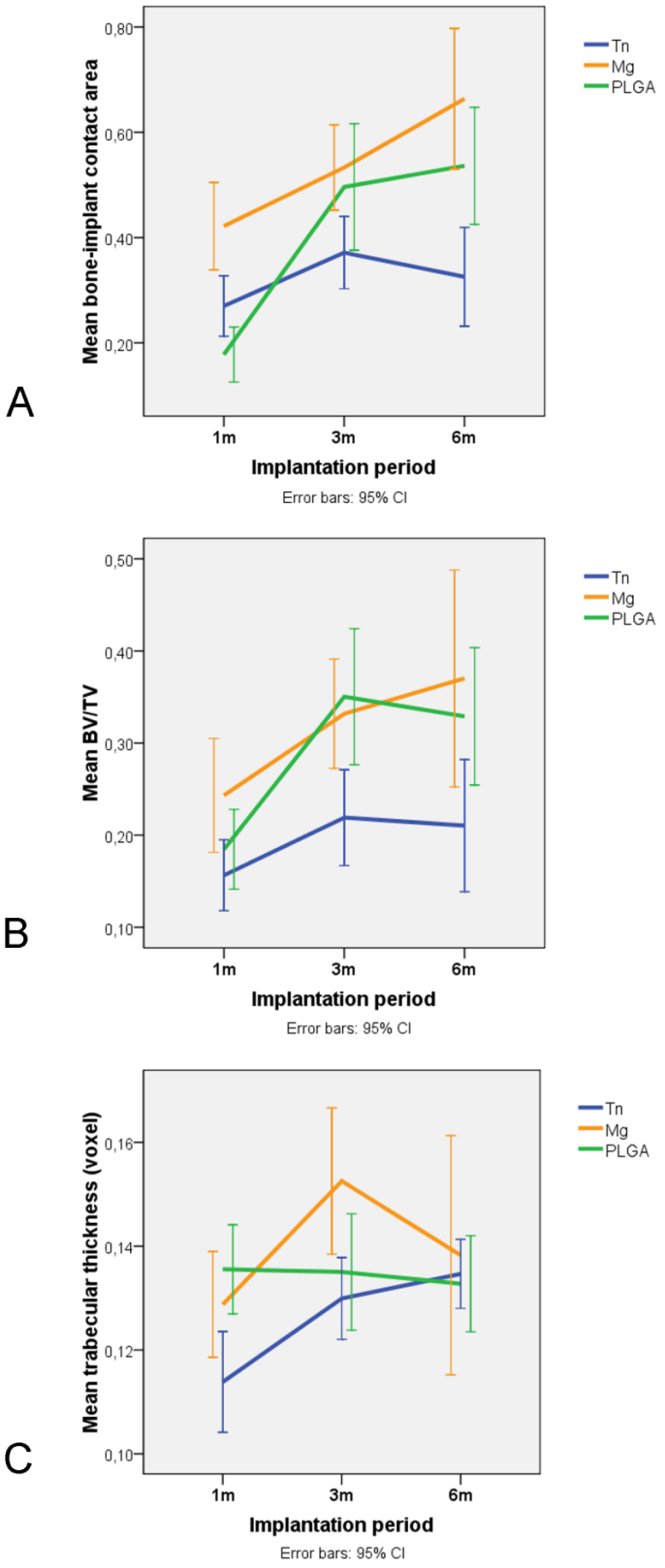

Figure 3-5. Mean (A) bone-implant contact area, (B) bone volume and (C) trabecular thickness after 1, 3 and 6 months of implantation

3.3 LIGHT MICROSCOPY AND SCANNING ELECTRON MICROSCOPY

After pushout testing, implant surfaces of all specimens were qualitatively examined by means of light microscopy. In addition, one Mg implant as well as one PLGA pin (both implanted for 1 month) were analysed using scanning electron microscopy.

In Mg implants, white areas were observed on the corroding pin surfaces which were supposed to represent newly formed bone growing into lacunae which resulted from surface degradation. The diameter and number of these regions seemed to augment with increasing implantation duration (Figure 3-6, B-H). In contrast, no such areas were found on the surface of Tn and PLGA implants.

Furthermore, the progressing degradation process was more obvious in Mg implants than in PLGA pins (Figure 3-6, B-H vs. C-I).

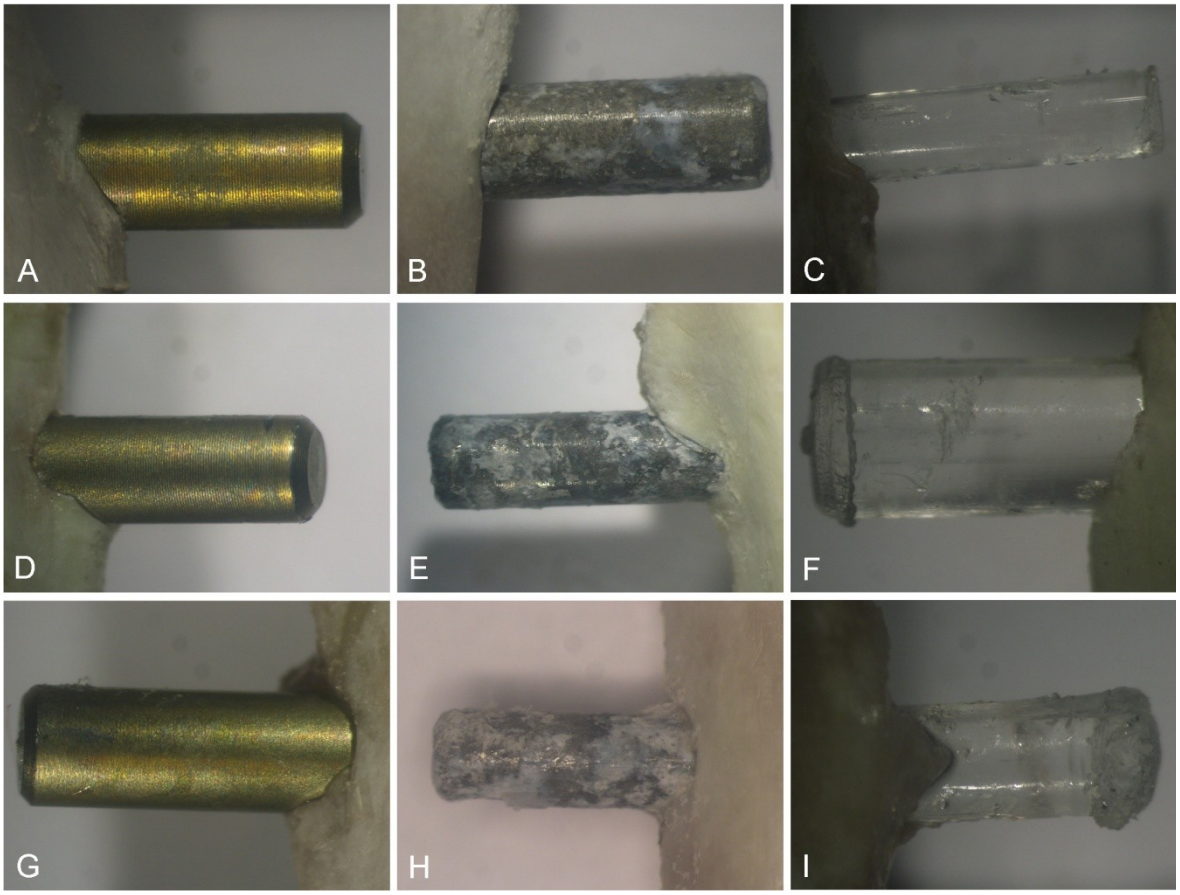

Figure 3-6. Light microscopic images of mechanically tested pins

Titanium **(A, D, G)**, Mg **(B, E, H)** and PLGA **(C, F, I)** implants after 1 **(A-C)**, 3 **(D-F)** and 6 **(G-I)** months of implantation

Scanning electron microscopy revealed that failure and debonding due to mechanical testing had occurred at the bone-implant interface (Figure 3-7, A and C). In addition, fissures and cracks were observed at the surface of the Mg implant, whereas the PLGA pin exhibited a smooth surface (Figure 3-7, B and D).

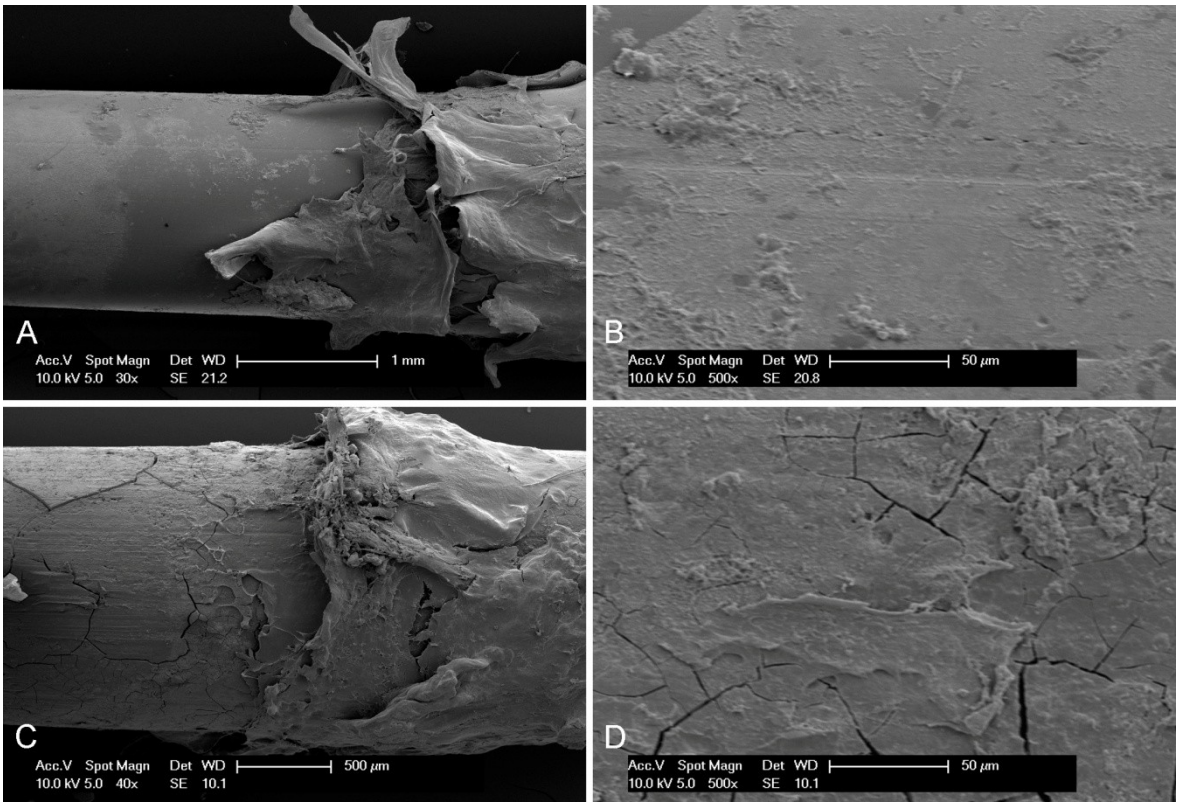

Figure 3-7. Scanning electron micrographs of mechanically tested pins after an implantation period of 1 month

(A) PLGA pin (original magnification x30), **(B)** PLGA pin (original magnification x500), **(C)** Mg pin (original magnification x40) and **(D)** Mg pin (original magnification x500)

3.4 FLUORESCENT LABELLING

Four different fluorochromes (Terramycin, Xylenolorange, Calcein and Calcein blue) were sequentially administered on day 14, 28, 56 and 84 postoperatively. 54 bone-implant specimens (6 per group) were examined and photographed in the fluorescence microscope at different wave lengths (Figure 3-8).

All fluorescent dyes were visible and could easily be discriminated. Each applied fluorochrome gave rise to a fluorescent band or rather areas at the bone-implant interface indicating new bone formation and active mineralization in vivo at different time intervals

However, the quantification of the amount of newly formed bone at the bone-implant interface per time period turned out to be very challenging and could not be achieved yet, but will be accomplished in the near future.

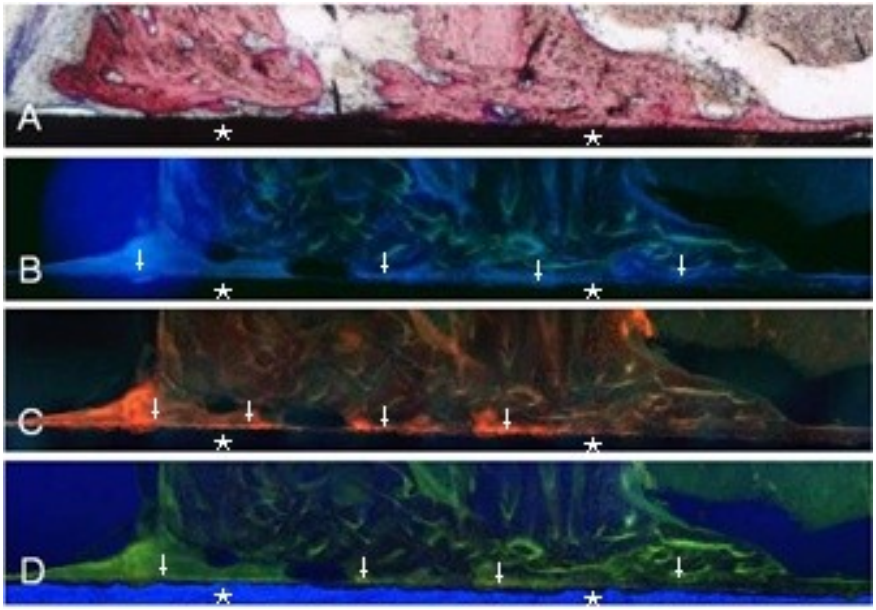

Figure 3-8. Fluorescence microscopic images of the bone-implant interface

(A) Histologic section and fluorescence images of the identical area showing fluorescent bands *(arrows)* of **(B)** calcein blue, **(C)** xylenolorange and **(D)** calcein; (Mg pin *(asterisks)*).

3.5 BLOOD PARAMETERS

Blood smears were performed from each animal at euthanasia after blood aspiration from the cardiac ventricle in order to detect potential systemic inflammatory reactions as a result of pin implantation. Table 3-12 summarises the collected data:

Table 3-12. Cellular distribution of different types of leucocytes for each implantation period and implant type (median, first and third quartile (in parentheses))

IP	IT	l-nGr [%]	s-nGr [%]	Mono [%]	Lympho [%]	eGr [%]	bGr [%]
1 m	Tn	14.50 (13.00-18.25)	0.50 (0.00-1.25)	10.00 (8.50-11.00)	72.00 (69.75-77.00)	1.00 (1.00-2.00)	0.00 (0.00-0.00)
	Mg	15.50 (12.25-18.75)	1.00 (0.00-1.75)	7.50 (3.25-10.00)	76.50 (71.25-79.00)	1.50 (0.25-2.00)	0.00 (0.00-0.00)
	PLGA	16.00 (13.00-20.00)	1.00 (0.25-1.75)	11.00 (5.25-12.00)	72.00 (66.75-76.00)	1.00 (0.25-2.00)	0.00 (0.00-0.75)
3 m	Tn	18.00 (15.50-20.50)	0.00 (0.00-0.05)	4.00 (3.00-7.00)	74.00 (72.50-78.50)	1.00 (0.00-1.50)	0.00 (0.00-0.50)
	Mg	16.00 (13.50-18.00)	0.00 (0.00-0.00)	3.00 (2.50-6.00)	80.00 (75.00-83.00)	1.00 (0.00-1.00)	0.00 (0.00-0.00)
	PLGA	12.50 (9.00-16.25)	0.50 (0.00-1.75)	10.50 (7.50-12.75)	74.00 (70.50-77.75)	1.00 (0.25-2.00)	0.00 (0.00-0.75)
6 m	Tn	15.00 (14.00-18.00)	0.00 (0.00-1.00)	14.00 (12.00-15.00)	71.00 (68.00-72.00)	0.00 (0.00-2.00)	0.00 (0.00-0.00)
	Mg	17.00 (15.00-22.25)	0.00 (0.00-1.00)	5.50 (3.75-8.00)	73.00 (71.00-80.00)	1.00 (0.00-1.25)	0.00 (0.00-0.25)
	PLGA	17.00 (14.50-19.00)	0.00 (0.00-1.00)	6.00 (4.50-6.50)	75.00 (74.50-78.00)	1.00 (0.00-2.00)	0.00 (0.00-0.00)

IP = implantation period; m = month(s); IT = implant type; l-nGr = lobulated neutrophil granulocytes, s-nGr = stab neutrophils, Mono= monocytes, Lympho = lymphocytes, eGr = eosinophil granulocytes, bGr = basophil granulocytes.

Differences among different implant types were detected after an implantation period of 3 and 6 months (Table 3-13).

Table 3-13. Differences in blood parameters among different implant types within each implantation period

IP	l-nGr[1]	s-nGr[2]	Mono[1]	Lympho[1]	eGr[2]	bGr[2]
1 m	0.904	0.579	0.308	0.404	0.770	0.533
3 m	0.004**	0.092	< 0.001**	0.074	0.546	0.834
6 m	0.204	0.820	< 0.001**	0.005**	0.812	0.189

[1] one-way ANOVA was conducted for normally distributed data: Welch one-way ANOVA in case of heterogeneous variances and one-way ANOVA if variances were homogenous; [2] non-normally distributed data were analysed using Kruskal-Wallis tests; * $p < 0.05$, ** $p < 0.01$; IP = implantation period; m = month(s); l-nGr = lobulated neutrophil granulocytes, s-nGr = stab neutrophils, Mono= monocytes, Lympho = lymphocytes, eGr = eosinophil granulocytes, bGr = basophil granulocytes.

Post hoc comparisons revealed that the mean percentage of lobulated neutrophil granulocytes was significantly lower in PLGA implants than in titanium implants ($p = 0.006$), whereas the percentage of monocytes was significantly higher in the former implants than in Mg ($p < 0.001$) as well as titanium ($p < 0.001$) pins after an implantation period of **3 months** (Table 3-14).

Among pins implanted for **6 months**, monocyte fraction was significantly greater in titanium implants than in Mg ($p < 0.001$) as well as in PLGA ($p < 0.001$) pins, whereas lymphocyte fraction was lower in titanium implants compared to PLGA ($p = 0.006$) and Mg ($p = 0.048$) pins.

Table 3-14. Pairwise comparisons of blood parameters between different implant types within each implantation period

Implantation Period	Analysed pairs	l-nGr[1]	s-nGr[2]	Mono[1]	Lympho[1]	eGr[2]	bGr[2]
1 month	Tn vs. Mg	NSGD	NSGD	NSGD	NSGD	NSGD	NSGD
	Tn vs. PLGA	NSGD	NSGD	NSGD	NSGD	NSGD	NSGD

	Mg vs. PLGA	NSGD	NSGD	NSGD	NSGD	NSGD	NSGD
3 months	Tn vs. Mg	0.504	NSGD	0.748	NSGD	NSGD	NSGD
	Tn vs. PLGA	0.006**	NSGD	< 0.001**	NSGD	NSGD	NSGD
	Mg vs. PLGA	0.054	NSGD	< 0.001**	NSGD	NSGD	NSGD
6 months	Tn vs. Mg	NSGD	NSGD	< 0.001**	0.048*	NSGD	NSGD
	Tn vs. PLGA	NSGD	NSGD	< 0.001**	0.006**	NSGD	NSGD
	Mg vs. PLGA	NSGD	NSGD	0.985	0.565	NSGD	NSGD

[1] Post hoc ANOVA was conducted for normally distributed data: Tamhane´s T2 post hoc tests in case of heterogeneous variances and Scheffe post hoc tests if variances were homogenous; [2] non-normally distributed data was analysed using Mann-Whitney U test; * $p < 0.05$, ** $p < 0.01$; NSGD = No significant differences in the previous one-way ANOVA; IP = implantation period; m = month(s); l-nGr = lobulated neutrophil granulocytes, s-nGr = stab neutrophils, Mono= monocytes, Lympho = lymphocytes, eGr = eosinophil granulocytes, bGr = basophil granulocytes.

4 DISCUSSION

Implants made of titanium or stainless steel as well as currently available bioabsorbable implants have specific drawbacks in clinical practice. The former have to be removed in a second operation (especially in paediatric trauma surgery) and are associated with stress shielding phenomenons [67,108], whereas the latter cause adverse tissue reactions[11,15,17-19,41,50] and exhibit limited mechanical properties [28,108]. Thus, new implant materials combining excellent strength retention properties, biodegradability and improved biocompatibility are desired. A new type of biodegradable implant made of a magnesium alloy has recently been developed and may be a potential candidate.

We therefore evaluated the biomechanical properties of the bone-implant interface as well as osseointegration of this novel implant by means of pushout testing, microfocus computed tomography, fluorescent labelling, lightmicroscopic and exemplary scanning electron microscopic examination of the tested implants after an implantation period of 1, 3 as well as 6 months. These findings were compared to those obtained for conventional titanium as well as new PLGA pins.

In this study in 102 male Sprague-Dawley rats, we have shown that these novel Mg implants exhibit highly significantly greater maximum pushout forces as well as ultimate shear strengths than titanium and PLGA pins after 1, 3 and 6 months of implantation, whereas Tn and PLGA demonstrated similar values. Furthermore, bone-implant contact area and bone volume were significantly higher in Mg implants than in titanium implants. Above all, no local or systemic inflammatory reactions were observed.

Pushout tests are widely used in implant-related orthopaedic research [7]. Although comparisons of pushout data obtained in different studies may be problematic, comparisons within one single experiment carried out under identical test conditions are valuable tools to assess mechanical fixation of orthopaedic devices in the surrounding bone [33]. Thus, we controlled potential confounding variables (e.g., implant dimension, surface roughness, implant composition, animal age, implanta-

tion site, alignment and mounting, fit of the support jig, displacement rate) thoroughly and great care was taken to standardise our experiments with regard to the recommendations published by Black[8]. We assessed four well established biomechanical parameters in order to characterise the mechanical properties of the bone-implant interface of the three different implants. However, interface stiffness could not be determined for PLGA implants after 1 and 3 months due to their irregular load-displacement curve progression (see Figure 4-1, E). The slope of the load-displacement curve could not be specified since there hardly existed any linear regions.

In contrast, the characteristic load-displacement curve progressions of titanium and Mg implants were similar (Figure 4-1, A-D): The initial linear segment of the curve reflected elastic deformation and was abruptly terminated after maximum pushout strength was reached. Thereafter pushout load gradually decreased. In Mg implants, the linear segment was followed by a short non-linear portion before F_{max} was attained, which was much less pronounced in titanium implants. This typical curve progression has been already described by several authors investigating metallic implants [20,21]. However, load-displacement curves of PLGA pins were less uniform and non-linear except for those after an implantation period of 6 months which showed nearly linear initial segments (Figure 4-1, F).

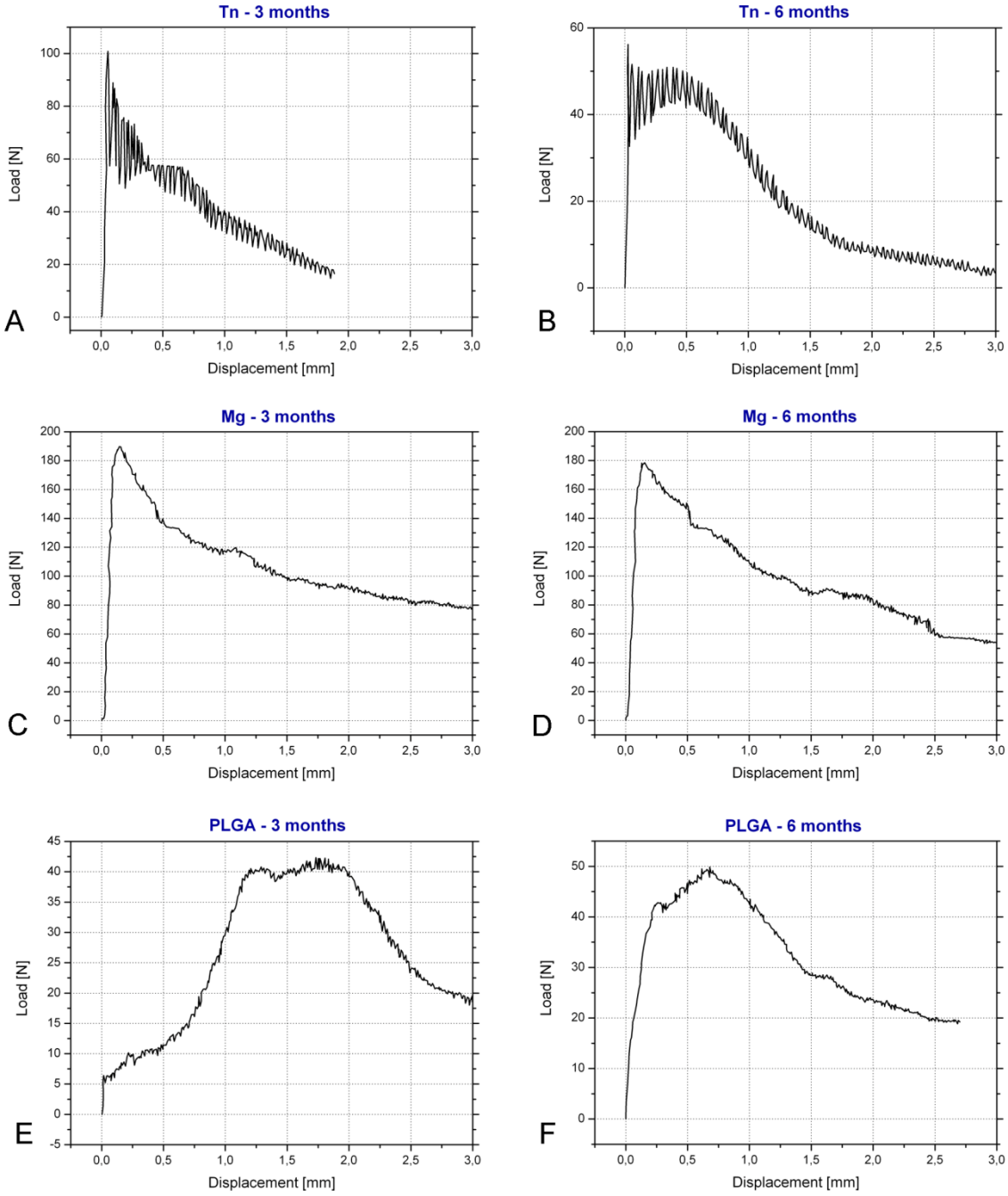

Figure 4-1. Load-displacement curves of titanium (A and B), Mg (C and D) and PLGA implants (E and F) after 3 (A, C and E) and 6 (B, D, F) months of implantation

Furthermore, in PLGA implants maximum pushout force was attained not until extensive pin displacement had occurred. For example, after 3 months of implantation in PLGA pins F_{max} was reached after median displacement of 1.86 mm com-

pared to 0.09 mm and 0.15 mm in Tn and Mg implants, respectively (see Appendix). In consequence, energy absorption to failure was much higher in PLGA pins. Thus, we are of the opinion that energy absorption to failure is no reliable tool to characterise mechanical attachment when comparing metal implants and polymers.

In addition, Dhert et al. [32] could show by means of finite element analyses that low Young´s modulus of implant causes less uniform stress distribution and hence tested implants should be of similar Young´s modulus. Nevertheless, we had to relate the biomechanical parameters obtained for PLGA pins to those of conventional titanium implants in order to receive an impression of implant fixation valuable for clinical practice.

Furthermore, loading of implants of low Young´s modulus may cause transverse elongation resulting in greater friction [89], in consequence maximum pushout force and ultimate shear strength may be overestimated. But even when referring to these potentially overestimated values, Mg implants yielded much greater implant fixation in the surrounding bone than PLGA pins, as we could demonstrate in this study. Several authors [3,4,110] evaluated implants made of bioabsorbable polymers by pushout tests, but to our knowledge none of them addressed the issue of transverse elongation of loaded polymers.

Mg implants yielded greatly higher maximum pushout force and ultimate shear strength values than titanium as well as PLGA implants after all three implantation periods. Ultimate shear strength was 2.2, 1.5 and 3.6-fold higher than in titanium and 3.5, 3.4 and 4.6-fold higher than in PLGA implants after an implantation period of 1, 3 and 6 months, respectively. Macroscopic and histologic observations may elucidate these findings: After pushout testing white areas were observed on the surface of Mg implants which were not present in titanium and PLGA pins. Hence, light microscopic examination of the pin surface of all implants was performed. Light microscopy further showed that the diameter and number of these white regions augmented with increasing implantation duration. We supposed these areas

to represent newly formed bone growing into lacunae which resulted from surface degradation or rather a newly formed mineral phase resulting from magnesium corrosion process as previously described by Witte et al. [119] . This assumption was supported by histomorphometric observations: As above mentioned, one femur of each rat was subjected to micro computed tomography, the other one was embedded for further histomorphometric (data not shown) and fluorescence microscopic analyses. Figure 4-2 shows a histologic section of a bone-implant specimen containing a Mg pin. The implant surface features irregular lacunae resulting from surface degradation. On the contrary, implant surface of PLGA pins seemed to remain quite smooth even after 6 months (Figure 3-6).

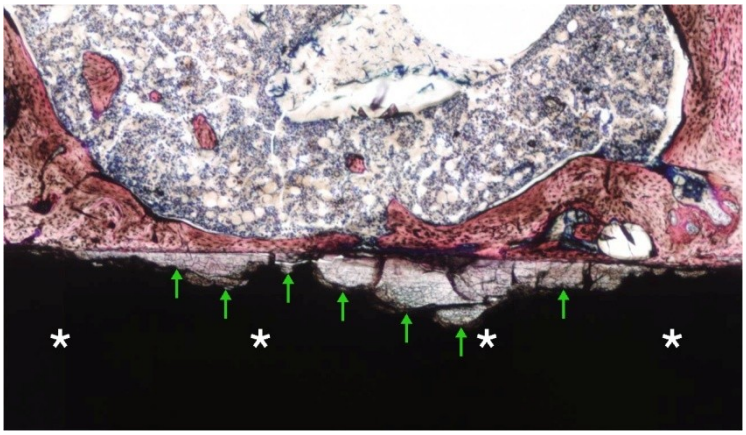

Figure 4-2. Histologic section of a Mg pin in the surrounding bone

The longitudinally sectioned Mg pin *(black area marked by white asterisks)* features a partially degraded surface. Thus, its outline is not anymore smooth but irregular shaped *(green arrows)*.

In a systematic review of animal studies, Shalabi et al. [94] investigated the influence of implant surface roughness on bone-implant integration. They provided evidence that increasing surface roughness enhances bone-implant contact. Furthermore, they addressed the question of whether surface roughness has an effect on biomechanical parameters in pushout testing. They stated that that all 5 studies dealing with this issue reported increased pushout strength in implants with higher surface roughness.

For instance, Wong et al. [122] placed cylindrical implants of 3 different surface textures in trabecular bone of mature minipigs. 12 weeks after implantation, pushout testing and histomorphometry were performed. Wong cited a rather high correlation (r2 = 0.90) between implant surface roughness and pushout failure load. Reviewing various data obtained from different biomechanical tests, Cooper [29] noted that the majority of these studies indicates that increasing implant surface roughness improves the mechanical attachment of the implant to the surrounding bone.
In addition, Thomas et al. [103] analysed 12 different implant types after 32 weeks of implantation in adult mongrel dogs and evaluated whether Young´s modulus (3 - 385 GPa), surface texture (polished vs. grit-blasted) or surface composition (uncoated vs. coated with ultra-low-temperature isotropic pyrolytic carbon) of these cylindrical implants significantly affect ultimate shear strength and bone apposition. Pushout testing revealed that neither Young´s modulus nor surface composition had an impact on ultimate shear strength or interface stiffness. Yet, they could demonstrate that pins with rougher surfaces showed higher shear strengths than the corresponding smooth surfaced implants of the same Young´s modulus.

With regard to these reports, superior maximum pushout force and ultimate shear strength of Mg pins may be at least partly attributed to higher surface roughness in consequence of their characteristic surface degradation.

It has to be noted that titanium implants unexpectedly exhibited lower median maximum pushout force and ultimate shear strength values after 6 months than after 3 months of implantation, even though this difference was not statistically significant. In contrast to our findings, Dalton et al. [30] found that interface attachment strength increased with time after implantation. Moreover, Branemark et al. [21] reported increasing pullout loads up to 16 weeks, albeit the observed increase was only moderate between 4 and 16 weeks of implantation. But contrary to our study, Branemark used threaded fixtures and tested in vivo, whereas Dalton evaluated an intramedullary placed porous bead coated titanium rod. Yet, studies performed under conditions similar to those of our experiments (uncoated, smooth cylindrical

titanium implants; implantation period up to 6 months; transcortical placement in the middiaphysis of the femur of rats; similar pushout test setup) are lacking in literature. Besides, as already mentioned above comparisons of pushout data obtained from different studies which were not conducted under identical conditions should be avoided, since there are numerous parameters which may affect results of pushout testing [8,33].
However, we do not so far have a satisfactory explanation for this decrease of pushout force and shear strength between 3 and 6 months of implantation.

In addition to mechanical testing microfocus computed tomography was utilised to evaluate osseointegration. This emerging imaging modality is non-destructive, less time-consuming, provides full three-dimensional data with a spatial resolution up to 5 µm and allows for two-dimensional image reconstruction in an arbitrary plane [35]. Moreover, it has already been validated as method for the assessment of trabecular [64,74,104] as well as cortical bone [5] and is increasingly used to study bone-implant integration.
We did not observe any substantial artefacts at the bone-implant interface in both the polymeric and the metallic implants, and were able to determine bone-implant contact area accurately using a 3 pixel thick ring as our region of interest. In contrast to our findings other groups reported considerable metal artefacts of titanium implants in microCT images:

Stoppie et al. [101] could not detect bone in a region 60 µm or closer to the titanium implant surface (Philips HOMX 161 microfocus x-ray system, isovoxel size: 24 µm) because of noise around the implant and stated that microfocus computed tomography is no reliable tool for bone-implant contact measurement around metal implants. Butz et al. [26] cited no significant correlation in the ratio of bone area to total area in close proximity to the implant (0 to 24 µm from implant surface) when comparing micro-computed tomography and histomorphometry, whereas the correlation between these techniques was significant for cancellous ($r = 0.92$, $p < 0.05$) as well as cortical ($r = 0.65$, $p < 0.05$) bone at distances of 24 to 240 µm from the surface of the pins. The author presumed that this lack of correlation may be

attributed to metal artefacts. In addition, Bernhardt et al. [6] concluded that microCT imaging roughly overestimates the amount of bone at distances of 200 µm and closer to the implant surface due to artefacts and beam hardening effects.

However, in accordance with our observations several investigators [43,56,63,88,109] found no substantial artefacts at the bone-implant interface and could precisely assess bone-implant contact area. For instance, Gabet et al. [43] investigated the effects of intermittently administered human parathyroid hormone 1–34 on osseointegration of smooth, threaded titanium implants (length: 5 mm, largest diameter: 0.9 mm) placed in the proximal tibial metaphysis of 37 Sprague-Dawley rats. They used a µCT40 imaging system (Scanco Medical, Bassersdorf, Switzerland) at a spatial nominal resolution of 15 µm and reported to be able to clearly depict and quantify bone-implant contact area.

The observed greater bone-implant contact area and BV/TV values in Mg implants may be explained by a potential osteoconductive effect of magnesium [100,120,123,124]. For instance, Witte et al. [119] implanted four rods of different magnesium alloys and a self-reinforced PLA pin into the medullary cavity of guinea pigs. They reported significantly enhanced mineralized bone area and mineral apposition rate in magnesium alloy implants compared to the PLA control. Thus, they hypothesised that a high concentration of magnesium ions at the bone-implant interface of magnesium alloy implants may result in activation of osteoblasts.

Furthermore, these authors described subcutaneous gas bubbles in consequence of the degradation process of the investigated magnesium alloy implants. The accumulated gas emerged within 1 week after implantation and vanished after 2 to 3 weeks. However, we did not observe such bubbles neither clinically nor in micro-computed tomography images.

Moreover, the performed blood examination at sacrifice did not indicate any systemic inflammatory reactions due to Mg pin implantation. This observation is in

accordance with Zhang et al. [127], who reported that white blood cell counts did not differ significantly before and after femoral implantation of a magnesium rod in rats. In addition, we did not find any inflammatory reactions adjacent to the implant. These findings are in agreement with good biocompatibility of magnesium implants reported by other investigators[100,120,121,127].

However, the main limitation of our study is that bone-implant integration, implant degradation and interfacial biomechanics were studied only up to 6 months although Mg and PLGA pins were just partly degraded. Thus, further research in adequate animal models (e.g., in sheep) is needed to clarify the long term (12 - 24 months) efficacy of these implants.

Nevertheless, this experimental study in rats clearly demonstrated that the investigated novel magnesium alloy implant exhibited superior bone-implant integration as well as significantly greater median maximum pushout force and ultimate shear strength than new PLGA and even than titanium pins. Furthermore, there was no evidence neither for local nor for systemic inflammatory reactions due to pin implantation. Finally, the results of this study leads us to the conclusion that the investigated magnesium alloy may be a very promising candidate for the design of new biodegradable fracture fixation devices in orthopaedic trauma surgery.

APPENDIX

Table 4-1. Pin displacement [mm] when reaching maximum pushout force for each implantation period and implant type (median, first and third quartile (in parentheses))

Implantation period	Implant type	Displacement at F_{max} [mm]
1 month	Tn	0.06 (0.04-0.06)
	Mg	0.06 (0.06-0.07)
	PLGA	1.66 (1.22-2.02)
3 months	Tn	0.09 (0.06-0.11)
	Mg	0.15 (0.10-0.17)
	PLGA	1.86 (1.51-2.20)
6 months	Tn	0.03 (0.02-0.06)
	Mg	0.19 (0.13-0.27)
	PLGA	0.65 (0.43-0.75)

Table 4-2. Global differences in displacement at F_{max} using Kruskal-Wallis-Tests (* p < 0.05, ** p < 0.01)

Implantation period	Displacement at F_{max}
1 month	< 0.001**
3 months	< 0.001**
6 months	< 0.001**

Table 4-3. Pair-wise analysis of global differences in displacement at F_{max} by Mann-Whitney-U-Tests with Bonferroni corrections (* p < 0.05, ** p < 0.01)

Implantation Period	Analysed pairs	Displacement at F_{max}
1 month	Tn vs. Mg	0.231
	Tn vs. PLGA	< 0.001**
	Mg vs. PLGA	< 0.001**
3 months	Tn vs. Mg	0.168
	Tn vs. PLGA	< 0.001**
	Mg vs. PLGA	< 0.001**
6 months	Tn vs. Mg	0.003**
	Tn vs. PLGA	< 0.001**
	Mg vs. PLGA	0.003**

REFERENCES

1. **Ahsan, T., and Sah, R. L.:** Biomechanics of integrative cartilage repair. *Osteoarthritis Cartilage,* 7(1): 29-40, 1999.
2. **Alan Barber, F.; Boothby, M. H.; and Richards, D. P.:** New sutures and suture anchors in sports medicine. *Sports Med Arthrosc,* 14(3): 177-84, 2006.
3. **An, Y. H.; Woolf, S. K.; and Friedman, R. J.:** Pre-clinical in vivo evaluation of orthopaedic bioabsorbable devices. *Biomaterials,* 21(24): 2635-52, 2000.
4. **Andriano, K. P.; Wenger, K. H.; Daniels, A. U.; and Heller, J.:** Technical note: biomechanical analysis of two absorbable fracture fixation pins after long-term canine implantation. *J Biomed Mater Res,* 48(4): 528-33, 1999.
5. **Basillais, A.; Bensamoun, S.; Chappard, C.; Brunet-Imbault, B.; Lemineur, G.; Ilharreborde, B.; Ho Ba Tho, M. C.; and Benhamou, C. L.:** Three-dimensional characterization of cortical bone microstructure by microcomputed tomography: validation with ultrasonic and microscopic measurements. *J Orthop Sci,* 12(2): 141-8, 2007.
6. **Bernhardt, R.; Scharnweber, D.; Muller, B.; Thurner, P.; Schliephake, H.; Wyss, P.; Beckmann, F.; Goebbels, J.; and Worch, H.:** Comparison of microfocus- and synchrotron X-ray tomography for the analysis of osteointegration around Ti6Al4V implants. *Eur Cell Mater,* 7: 42-51; discussion 51, 2004.
7. **Berzins, A., and Sumner, D. R.:** Implant Pushout and Pullout Tests. In *Mechanical Testing of Bone and the Bone-Implant Interface*. Edited by An, Y. H., and Draughn, R. A., Boca Raton, USA, CRC Press, 1999.
8. **Black, J.:** "Push-out" tests. *J Biomed Mater Res,* 23(11): 1243-5, 1989.
9. **Bohnsack, M.; Borner, C.; Schmolke, S.; Moller, H.; Wirth, C. J.; and Ruhmann, O.:** Clinical results of arthroscopic meniscal repair using biodegradable screws. *Knee Surg Sports Traumatol Arthrosc,* 11(6): 379-83, 2003.
10. **Borchers, R. E.; Gibson, L. J.; Burchardt, H.; and Hayes, W. C.:** Effects of selected thermal variables on the mechanical properties of trabecular bone. *Biomaterials,* 16(7): 545-51, 1995.
11. **Bostman, O.; Hirvensalo, E.; Makinen, J.; and Rokkanen, P.:** Foreign-body reactions to fracture fixation implants of biodegradable synthetic polymers. *J Bone Joint Surg Br,* 72(4): 592-6, 1990.
12. **Bostman, O.; Hirvensalo, E.; Partio, E.; Tormala, P.; and Rokkanen, P.:** Impact of the use of absorbable fracture fixation implants on consumption of hospital resources and economic costs. *J Trauma,* 31(10): 1400-3, 1991.

13. **Bostman, O.; Makela, E. A.; Sodergard, J.; Hirvensalo, E.; Tormala, P.; and Rokkanen, P.:** Absorbable polyglycolide pins in internal fixation of fractures in children. *J Pediatr Orthop,* 13(2): 242-5, 1993.

14. **Bostman, O.; Makela, E. A.; Tormala, P.; and Rokkanen, P.:** Transphyseal fracture fixation using biodegradable pins. *J Bone Joint Surg Br,* 71(4): 706-7, 1989.

15. **Bostman, O., and Pihlajamaki, H.:** Clinical biocompatibility of biodegradable orthopaedic implants for internal fixation: a review. *Biomaterials,* 21(24): 2615-21, 2000.

16. **Bostman, O. M.:** Metallic or absorbable fracture fixation devices. A cost minimization analysis. *Clin Orthop Relat Res,* (329): 233-9, 1996.

17. **Bostman, O. M.:** Osteoarthritis of the ankle after foreign-body reaction to absorbable pins and screws: a three- to nine-year follow-up study. *J Bone Joint Surg Br,* 80(2): 333-8, 1998.

18. **Bostman, O. M.:** Osteolytic changes accompanying degradation of absorbable fracture fixation implants. *J Bone Joint Surg Br,* 73(4): 679-82, 1991.

19. **Bostman, O. M., and Pihlajamaki, H. K.:** Adverse tissue reactions to bioabsorbable fixation devices. *Clin Orthop Relat Res,* (371): 216-27, 2000.

20. **Brandt, J.; Bierogel, C.; Holweg, K.; Hein, W.; and Grellmann, W.:** [Extended push-out test to characterize the failure of bone-implant interface]. *Biomed Tech (Berl),* 50(6): 201-6, 2005.

21. **Branemark, R.; Ohrnell, L. O.; Nilsson, P.; and Thomsen, P.:** Biomechanical characterization of osseointegration during healing: an experimental in vivo study in the rat. *Biomaterials,* 18(14): 969-78, 1997.

22. **Branemark, R.; Ohrnell, L. O.; Skalak, R.; Carlsson, L.; and Branemark, P. I.:** Biomechanical characterization of osseointegration: an experimental in vivo investigation in the beagle dog. *J Orthop Res,* 16(1): 61-9, 1998.

23. **Branemark, R., and Skalak, R.:** An in-vivo method for biomechanical characterization of bone-anchored implants. *Med Eng Phys,* 20(3): 216-9, 1998.

24. **Bucholz, R. W.; Henry, S.; and Henley, M. B.:** Fixation with bioabsorbable screws for the treatment of fractures of the ankle. *J Bone Joint Surg Am,* 76(3): 319-24, 1994.

25. **Burkhart, S. S.:** The evolution of clinical applications of biodegradable implants in arthroscopic surgery. *Biomaterials,* 21(24): 2631-4, 2000.

26. **Butz, F.; Ogawa, T.; Chang, T. L.; and Nishimura, I.:** Three-dimensional bone-implant integration profiling using micro-computed tomography. *Int J Oral Maxillofac Implants,* 21(5): 687-95, 2006.

27. **Ciccone, W. J., 2nd; Motz, C.; Bentley, C.; and Tasto, J. P.:** Bioabsorbable implants in orthopaedics: new developments and clinical applications. *J Am Acad Orthop Surg,* 9(5): 280-8, 2001.

28. **Claes, L., and Ignatius, A.:** [Development of new, biodegradable implants]. *Chirurg,* 73(10): 990-6, 2002.

29. **Cooper, L. F.:** A role for surface topography in creating and maintaining bone at titanium endosseous implants. *J Prosthet Dent,* 84(5): 522-34, 2000.

30. **Dalton, J. E.; Cook, S. D.; Thomas, K. A.; and Kay, J. F.:** The effect of operative fit and hydroxyapatite coating on the mechanical and biological response to porous implants. *J Bone Joint Surg Am,* 77(1): 97-110, 1995.

31. **Davies, J. E.:** Mechanisms of endosseous integration. *Int J Prosthodont,* 11(5): 391-401, 1998.

32. **Dhert, W. J.; Verheyen, C. C.; Braak, L. H.; de Wijn, J. R.; Klein, C. P.; de Groot, K.; and Rozing, P. M.:** A finite element analysis of the push-out test: influence of test conditions. *J Biomed Mater Res,* 26(1): 119-30, 1992.

33. **Dhert, W. J. A., and Jansen, J. A.:** The Validity of a Single Pushout Test. In *Mechanical Testing of Bone and the Bone-Implant Interface*. Edited by An, Y. H., and Draughn, R. A., Boca Raton, USA, CRC Press, 1999.

34. **Eglin, D., and Alini, M.:** Degradable polymeric materials for osteosynthesis: tutorial. *Eur Cell Mater,* 16: 80-91, 2008.

35. **Engelke, K.; Karolczak, M.; Lutz, A.; Seibert, U.; Schaller, S.; and Kalender, W.:** [Micro-CT. Technology and application for assessing bone structure]. *Radiologe,* 39(3): 203-12, 1999.

36. **Eppley, B. L.:** Use of resorbable plates and screws in pediatric facial fractures. *J Oral Maxillofac Surg,* 63(3): 385-91, 2005.

37. **Eppley, B. L.; Sadove, A. M.; and Havlik, R. J.:** Resorbable plate fixation in pediatric craniofacial surgery. *Plast Reconstr Surg,* 100(1): 1-7; discussion 8-13, 1997.

38. **Fedorowicz, Z.; Nasser, M.; Newton, J. T.; and Oliver, R. J.:** Resorbable versus titanium plates for orthognathic surgery. *Cochrane Database Syst Rev,* (2): CD006204, 2007.

39. **Fink, C.; Benedetto, K. P.; Hackl, W.; Hoser, C.; Freund, M. C.; and Rieger, M.:** Bioabsorbable polyglyconate interference screw fixation in anterior cruciate ligament reconstruction: a prospective computed tomography-controlled study. *Arthroscopy,* 16(5): 491-8, 2000.

40. **Franchi, M.; Fini, M.; Martini, D.; Orsini, E.; Leonardi, L.; Ruggeri, A.; Giavaresi, G.; and Ottani, V.:** Biological fixation of endosseous implants. *Micron,* 36(7-8): 665-71, 2005.

41. **Fraser, R. K., and Cole, W. G.:** Osteolysis after biodegradable pin fixation of fractures in children. *J Bone Joint Surg Br,* 74(6): 929-30, 1992.

42. **Fuchs, M.; Vosshenrich, R.; Dumont, C.; and Sturmer, K. M.:** [Refixation of osteochondral fragments using absorbable implants. First results of a retrospective study]. *Chirurg,* 74(6): 554-61, 2003.

43. **Gabet, Y.; Muller, R.; Levy, J.; Dimarchi, R.; Chorev, M.; Bab, I.; and Kohavi, D.:** Parathyroid hormone 1-34 enhances titanium implant anchorage in low-density trabecular bone: a correlative micro-computed tomographic and biomechanical analysis. *Bone,* 39(2): 276-82, 2006.

44. **Gogolewski, S.:** Bioresorbable polymers in trauma and bone surgery. *Injury,* 31 Suppl 4: 28-32, 2000.

45. **Goh, J. C.; Ang, E. J.; and Bose, K.:** Effect of preservation medium on the mechanical properties of cat bones. *Acta Orthop Scand,* 60(4): 465-7, 1989.

46. **Griffon, D. J.; Wallace, L. J.; and Bechtold, J. E.:** Biomechanical properties of canine corticocancellous bone frozen in normal saline solution. *Am J Vet Res,* 56(6): 822-5, 1995.

47. **Gunja, N. J., and Athanasiou, K. A.:** Biodegradable materials in arthroscopy. *Sports Med Arthrosc,* 14(3): 112-9, 2006.

48. **Harrigan, T. P.; Kareh, J.; and Harris, W. H.:** The influence of support conditions in the loading fixture on failure mechanisms in the push-out test: a finite element study. *J Orthop Res,* 8(5): 678-84, 1990.

49. **Hirvensalo, E.; Bostman, O.; and Rokkanen, P.:** Absorbable polyglycolide pins in fixation of displaced fractures of the radial head. *Arch Orthop Trauma Surg,* 109(5): 258-61, 1990.

50. **Hoffmann, R.; Weller, A.; Helling, H. J.; Krettek, C.; and Rehm, K. E.:** [Local foreign body reactions to biodegradable implants. A classification]. *Unfallchirurg,* 100(8): 658-66, 1997.

51. **Hope, P. G.; Williamson, D. M.; Coates, C. J.; and Cole, W. G.:** Biodegradable pin fixation of elbow fractures in children. A randomised trial. *J Bone Joint Surg Br,* 73(6): 965-8, 1991.

52. **Hughes, T. B.:** Bioabsorbable implants in the treatment of hand fractures: an update. *Clin Orthop Relat Res,* 445: 169-74, 2006.

53. **Huss, B. T.; Anderson, M. A.; Wagner-Mann, C. C.; and Payne, J. T.:** Effects of temperature and storage time on pin pull-out testing in harvested canine femurs. *Am J Vet Res,* 56(6): 715-9, 1995.

54. **Johnson, A. L.; Moutray, M.; and Hoffmann, W. E.:** Effect of ethylene oxide sterilization and storage conditions on canine cortical bone harvested for banking. *Vet Surg,* 16(6): 418-22, 1987.

55. **Jukkala-Partio, K.; Partio, E. K.; Hirvensalo, E.; and Rokkanen, P.:** Absorbable fixation of femoral head fractures. A prospective study of six cases. *Ann Chir Gynaecol,* 87(1): 44-8, 1998.

56. **Jung, H.; Kim, H. J.; Hong, S.; Kim, K. D.; Moon, H. S.; Je, J. H.; and Hwu, Y.:** Osseointegration assessment of dental implants using a synchrotron radiation imaging technique: a preliminary study. *Int J Oral Maxillofac Implants,* 18(1): 121-6, 2003.

57. **Kaeding, C.; Farr, J.; Kavanaugh, T.; and Pedroza, A.:** A prospective randomized comparison of bioabsorbable and titanium anterior cruciate ligament interference screws. *Arthroscopy,* 21(2): 147-51, 2005.

58. **Kang, J. S., and Kim, N. H.:** The biomechanical properties of deep freezing and freeze drying bones and their biomechanical changes after in-vivo allograft. *Yonsei Med J,* 36(4): 332-5, 1995.

59. **Kang, Q.; An, Y. H.; and Friedman, R. J.:** Effects of multiple freezing-thawing cycles on ultimate indentation load and stiffness of bovine cancellous bone. *Am J Vet Res,* 58(10): 1171-3, 1997.

60. **Kankare, J.:** Operative treatment of displaced intra-articular fractures of the calcaneus using absorbable internal fixation: a prospective study of twenty-five fractures. *J Orthop Trauma,* 12(6): 413-9, 1998.

61. **Kankare, J.:** Tibial condylar fractures fixed with totally absorbable, self-reinforced polyglycolide screws. A preliminary report. *Arch Orthop Trauma Surg,* 116(3): 133-6, 1997.

62. **Kankare, J., and Rokkanen, P.:** Dislocated fractures of the talus treated with biodegradable internal fixation. *Arch Orthop Trauma Surg,* 117(1-2): 62-4, 1998.

63. **Kiba, H.; Hayakawa, T.; Oba, S.; Kuwabara, M.; Habata, I.; and Yamamoto, H.:** Potential application of high-resolution microfocus X-ray techniques for observation of bone structure and bone-implant interface. *Int J Oral Maxillofac Implants,* 18(2): 279-85, 2003.

64. **Kuhn, J. L.; Goldstein, S. A.; Feldkamp, L. A.; Goulet, R. W.; and Jesion, G.:** Evaluation of a microcomputed tomography system to study trabecular bone structure. *J Orthop Res,* 8(6): 833-42, 1990.

65. **Laitinen, M.; Kivikari, R.; and Hirn, M.:** Lipid oxidation may reduce the quality of a fresh-frozen bone allograft. Is the approved storage temperature too high? *Acta Orthop,* 77(3): 418-21, 2006.

66. **Linde, F., and Sorensen, H. C.:** The effect of different storage methods on the mechanical properties of trabecular bone. *J Biomech,* 26(10): 1249-52, 1993.

67. **Litsky, A. S.:** Clinical reviews: bioabsorbable implants for orthopaedic fracture fixation. *J Appl Biomater,* 4(1): 109-11, 1993.

68. **Makela, E. A.; Bostman, O.; Kekomaki, M.; Sodergard, J.; Vainio, J.; Tormala, P.; and Rokkanen, P.:** Biodegradable fixation of distal humeral physeal fractures. *Clin Orthop Relat Res,* (283): 237-43, 1992.

69. **Makela, E. A.; Vainionpaa, S.; Vihtonen, K.; Mero, M.; Helevirta, P.; Tormala, P.; and Rokkanen, P.:** The effect of a penetrating biodegradable implant on the growth plate. An experimental study on growing rabbits with special reference to polydioxanone. *Clin Orthop Relat Res,* (241): 300-8, 1989.

70. **Marco, F.; Milena, F.; Gianluca, G.; and Vittoria, O.:** Peri-implant osteogenesis in health and osteoporosis. *Micron,* 36(7-8): 630-44, 2005.

71. **Matter, H. P.; Garrel, T. V.; Bilderbeek, U.; and Mittelmeier, W.:** Biomechanical examinations of cancellous bone concerning the influence of duration and temperature of cryopreservation. *J Biomed Mater Res,* 55(1): 40-4, 2001.

72. **McKoy, B. E.; An, Y. H.; and Friedman, R. J.:** Factors Affecting the Strength of the Bone-Implant Interface. In *Mechanical Testing of Bone and the Bone-Implant Interface*. Edited by An, Y. H., and Draughn, R. A., Boca Raton, USA, CRC Press, 1999.

73. **Middleton, J. C., and Tipton, A. J.:** Synthetic biodegradable polymers as orthopedic devices. *Biomaterials,* 21(23): 2335-46, 2000.

74. **Muller, R.; Van Campenhout, H.; Van Damme, B.; Van Der Perre, G.; Dequeker, J.; Hildebrand, T.; and Ruegsegger, P.:** Morphometric analysis of human bone biopsies: a quantitative structural comparison of histological sections and micro-computed tomography. *Bone,* 23(1): 59-66, 1998.

75. **Nakamura, T. a., and Nishiguchi, S.:** Tensile Testing of Bone-Implant Interface. In *Mechanical Testing of Bone and the Bone-Implant Interface*. Edited by An, Y. H., and Draughn, R. A., Boca Raton, USA, CRC Press, 1999.

76. **Nurmi, J. T.; Koho, P.; Ahvenj„rvi, P.; Suuriniemi, N.; and Ulmanen, M.:** Biomechanical testing of the Inion OTPS (TM) biodegradable fixation system; Poster presentation Inion Ltd, Finland. 2006.

77. **Panjabi, M. M.; Krag, M.; Summers, D.; and Videman, T.:** Biomechanical time-tolerance of fresh cadaveric human spine specimens. *J Orthop Res,* 3(3): 292-300, 1985.

78. **Partio, E. K.; Hirvensalo, E.; Bostman, O.; Patiala, H.; Vainionpaa, S.; Vihtonen, R.; Helevirta, P.; Tormala, P.; and Rokkanen, P.:** [Absorbable rods and screws: a new method of fixation for fractures of the olecranon]. *Int Orthop,* 16(3): 250-4, 1992.

79. **Partio, E. K.; Tuompo, P.; Hirvensalo, E.; Bostman, O.; and Rokkanen, P.:** Totally absorbable fixation in the treatment of fractures of the distal femoral epiphyses. A prospective clinical study. *Arch Orthop Trauma Surg,* 116(4): 213-6, 1997.

80. **Paulus, M. J.; Gleason, S. S.; Easterly, M. E.; and Foltz, C. J.:** A review of high-resolution X-ray computed tomography and other imaging modalities for small animal research. *Lab Anim (NY),* 30(3): 36-45, 2001.

81. **Pautke, C.; Tischer, T.; Vogt, S.; Haczek, C.; Deppe, H.; Neff, A.; Horch, H. H.; Schieker, M.; and Kolk, A.:** New advances in fluorochrome sequential labelling of teeth using seven different fluorochromes and spectral image analysis. *J Anat,* 210(1): 117-21, 2007.

82. **Pautke, C.; Vogt, S.; Tischer, T.; Wexel, G.; Deppe, H.; Milz, S.; Schieker, M.; and Kolk, A.:** Polychrome labeling of bone with seven different

fluorochromes: enhancing fluorochrome discrimination by spectral image analysis. *Bone,* 37(4): 441-5, 2005.

83. **Pelker, R. R.; Friedlaender, G. E.; Markham, T. C.; Panjabi, M. M.; and Moen, C. J.:** Effects of freezing and freeze-drying on the biomechanical properties of rat bone. *J Orthop Res,* 1(4): 405-11, 1984.

84. **Pelto-Vasenius, K.; Hirvensalo, E.; Vasenius, J.; Partio, E. K.; Bostman, O.; and Rokkanen, P.:** Redisplacement after ankle osteosynthesis with absorbable implants. *Arch Orthop Trauma Surg,* 117(3): 159-62, 1998.

85. **Pelto, K.; Hirvensalo, E.; Bostman, O.; and Rokkanen, P.:** Treatment of radial head fractures with absorbable polyglycolide pins: a study on the security of the fixation in 38 cases. *J Orthop Trauma,* 8(2): 94-8, 1994.

86. **Pereira, B. P.; Khong, K. S.; and Ng, R. T.:** The effect of storage at -70 degrees C and -150 degrees C on the torsion properties of the canine femur. *Ann Acad Med Singapore,* 28(1): 37-43, 1999.

87. **Petsche, T. S.; Selesnick, H.; and Rochman, A.:** Arthroscopic meniscus repair with bioabsorbable arrows. *Arthroscopy,* 18(3): 246-53, 2002.

88. **Rebaudi, A.; Koller, B.; Laib, A.; and Trisi, P.:** Microcomputed tomographic analysis of the peri-implant bone. *Int J Periodontics Restorative Dent,* 24(4): 316-25, 2004.

89. **Rödhammer, M.:** Interface Bindung und Biokompatibilität von Kieferimplantaten; Diploma Thesis, Institute of Solid State Physics, Vienna University of Technology, 2000.

90. **Roe, S. C.; Pijanowski, G. J.; and Johnson, A. L.:** Biomechanical properties of canine cortical bone allografts: effects of preparation and storage. *Am J Vet Res,* 49(6): 873-7, 1988.

91. **Rokkanen, P.; Bostman, O.; Vainionpaa, S.; Makela, E. A.; Hirvensalo, E.; Partio, E. K.; Vihtonen, K.; Patiala, H.; and Tormala, P.:** Absorbable devices in the fixation of fractures. *J Trauma,* 40(3 Suppl): S123-7, 1996.

92. **Salai, M.; Brosh, T.; Keller, N.; Perelman, M.; and Dudkiewitz, I.:** The effects of prolonged cryopreservation on the biomechanical properties of bone allografts: a microbiological, histological and mechanical study. *Cell Tissue Bank,* 1(1): 69-73, 2000.

93. **Santavirta, S.; Konttinen, Y. T.; Saito, T.; Gronblad, M.; Partio, E.; Kemppinen, P.; and Rokkanen, P.:** Immune response to polyglycolic acid implants. *J Bone Joint Surg Br,* 72(4): 597-600, 1990.

94. **Shalabi, M. M.; Gortemaker, A.; Van't Hof, M. A.; Jansen, J. A.; and Creugers, N. H.:** Implant surface roughness and bone healing: a systematic review. *J Dent Res,* 85(6): 496-500, 2006.

95. **Shirazi-Adl, A.:** Finite element stress analysis of a push-out test. Part 1: Fixed interface using stress compatible elements. *J Biomech Eng,* 114(1): 111-8, 1992.

96. **Shirazi-Adl, A., and Forcione, A.:** Finite element stress analysis of a push-out test. Part II: Free interface with nonlinear friction properties. *J Biomech Eng,* 114(2): 155-61, 1992.

97. **Simonian, P. T.; Conrad, E. U.; Chapman, J. R.; Harrington, R. M.; and Chansky, H. A.:** Effect of sterilization and storage treatments on screw pullout strength in human allograft bone. *Clin Orthop Relat Res,* (302): 290-6, 1994.

98. **Sinisaari, I. P.; Luthje, P. M.; and Mikkonen, R. H.:** Ruptured tibio-fibular syndesmosis: comparison study of metallic to bioabsorbable fixation. *Foot Ankle Int,* 23(8): 744-8, 2002.

99. **Slongo, T. F.:** The potential for bioresorbable implants in paediatric fractures. *Injury,* 33 Suppl 2: B84-7, 2002.

100. **Staiger, M. P.; Pietak, A. M.; Huadmai, J.; and Dias, G.:** Magnesium and its alloys as orthopedic biomaterials: a review. *Biomaterials,* 27(9): 1728-34, 2006.

101. **Stoppie, N.; van der Waerden, J. P.; Jansen, J. A.; Duyck, J.; Wevers, M.; and Naert, I. E.:** Validation of microfocus computed tomography in the evaluation of bone implant specimens. *Clin Implant Dent Relat Res,* 7(2): 87-94, 2005.

102. **Stoppie, N.; Wevers, M.; and Naert, I.:** Feasibility of detecting trabecular bone around percutaneous titanium implants in rabbits by in vivo microfocus computed tomography. *J Microsc,* 228(Pt 1): 55-61, 2007.

103. **Thomas, K. A., and Cook, S. D.:** An evaluation of variables influencing implant fixation by direct bone apposition. *J Biomed Mater Res,* 19(8): 875-901, 1985.

104. **Thomsen, J. S.; Laib, A.; Koller, B.; Prohaska, S.; Mosekilde, L.; and Gowin, W.:** Stereological measures of trabecular bone structure: comparison of 3D micro computed tomography with 2D histological sections in human proximal tibial bone biopsies. *J Microsc,* 218(Pt 2): 171-9, 2005.

105. **Tormala, P.:** Biodegradable self-reinforced composite materials; manufacturing structure and mechanical properties. *Clin Mater,* 10(1-2): 29-34, 1992.

106. **Tsai, A. M.; McAllister, D. R.; Chow, S.; Young, C. R.; and Hame, S. L.:** Results of meniscal repair using a bioabsorbable screw. *Arthroscopy,* 20(6): 586-90, 2004.

107. **Tuompo, P.; Partio, E. K.; Jukkala-Partio, K.; Pohjonen, T.; Helevirta, P.; and Rokkanen, P.:** Comparison of polylactide screw and expansion bolt in bioabsorbable fixation with patellar tendon bone graft for anterior cruciate ligament rupture of the knee. A preliminary study. *Knee Surg Sports Traumatol Arthrosc,* 7(5): 296-302, 1999.

108. **van Elst, M.:** [Biologically degradable implants in trauma surgery]. *Unfallchirurg,* 103(3): 177, 2000.

109. **Van Oossterwyck, H.; Duyck, J.; Vander Sloten, J.; Van der Perre, G.; Jansen, J.; Wevers, M.; and Naert, I.:** Use of microfocus computerized tomography as a new technique for characterizing bone tissue around oral implants. *J Oral Implantol,* 26(1): 5-12, 2000.

110. **Verheyen, C. C.; de Wijn, J. R.; van Blitterswijk, C. A.; de Groot, K.; and Rozing, P. M.:** Hydroxylapatite/poly(L-lactide) composites: an animal study on push-out strengths and interface histology. *J Biomed Mater Res,* 27(4): 433-44, 1993.

111. **Viceconti, M.; Monti, L.; Muccini, R.; Bernakiewicz, M.; and Toni, A.:** Even a thin layer of soft tissue may compromise the primary stability of cementless hip stems. *Clin Biomech (Bristol, Avon),* 16(9): 765-75, 2001.

112. **Voggenreiter, G.; Ascherl, R.; Blumel, G.; and Schmit-Neuerburg, K. P.:** Effects of preservation and sterilization on cortical bone grafts. A scanning electron microscopic study. *Arch Orthop Trauma Surg,* 113(5): 294-6, 1994.

113. **Voggenreiter, G.; Ascherl, R.; Fruh, H. J.; Blumel, G.; and Schmit-Neuerburg, K. P.:** [Preservation and sterilization of cortical bone--biomechanical studies of the rat]. *Unfallchirurg,* 98(2): 53-8, 1995.

114. **Walsh, S. J.; Boyle, M. J.; and Morganti, V.:** Large osteochondral fractures of the lateral femoral condyle in the adolescent: outcome of bioabsorbable pin fixation. *J Bone Joint Surg Am,* 90(7): 1473-8, 2008.

115. **Waris, E.; Ashammakhi, N.; Kaarela, O.; Raatikainen, T.; and Vasenius, J.:** Use of bioabsorbable osteofixation devices in the hand. *J Hand Surg [Br],* 29(6): 590-8, 2004.

116. **Warme, W. J.; Arciero, R. A.; Savoie, F. H., 3rd; Uhorchak, J. M.; and Walton, M.:** Nonabsorbable versus absorbable suture anchors for open Bankart repair. A prospective, randomized comparison. *Am J Sports Med,* 27(6): 742-6, 1999.

117. **Weiler, A.; Hoffmann, R. F.; Stahelin, A. C.; Helling, H. J.; and Sudkamp, N. P.:** Biodegradable implants in sports medicine: the biological base. *Arthroscopy,* 16(3): 305-21, 2000.

118. **Wingerter, S.; Calvert, G.; Tucci, M.; Benghuzzi, H.; Russell, G.; and Puckett, A.:** Mechanical strength repercussions of various fixative storage methods on bone. *Biomed Sci Instrum,* 42: 290-5, 2006.

119. **Witte, F.; Kaese, V.; Haferkamp, H.; Switzer, E.; Meyer-Lindenberg, A.; Wirth, C. J.; and Windhagen, H.:** In vivo corrosion of four magnesium alloys and the associated bone response. *Biomaterials,* 26(17): 3557-63, 2005.

120. **Witte, F.; Ulrich, H.; Palm, C.; and Willbold, E.:** Biodegradable magnesium scaffolds: Part II: peri-implant bone remodeling. *J Biomed Mater Res A,* 81(3): 757-65, 2007.

121. **Witte, F.; Ulrich, H.; Rudert, M.; and Willbold, E.:** Biodegradable magnesium scaffolds: Part 1: appropriate inflammatory response. *J Biomed Mater Res A,* 81(3): 748-56, 2007.

122. **Wong, M.; Eulenberger, J.; Schenk, R.; and Hunziker, E.:** Effect of surface topology on the osseointegration of implant materials in trabecular bone. *J Biomed Mater Res,* 29(12): 1567-75, 1995.

123. **Yamasaki, Y.; Yoshida, Y.; Okazaki, M.; Shimazu, A.; Kubo, T.; Akagawa, Y.; and Uchida, T.:** Action of FGMgCO3Ap-collagen composite in promoting bone formation. *Biomaterials,* 24(27): 4913-20, 2003.

124. **Yamasaki, Y. et al.:** Synthesis of functionally graded MgCO3 apatite accelerating osteoblast adhesion. *J Biomed Mater Res,* 62(1): 99-105, 2002.

125. **Yaszemski, M. J.; Payne, R. G.; Hayes, W. C.; Langer, R.; and Mikos, A. G.:** In vitro degradation of a poly(propylene fumarate)-based composite material. *Biomaterials,* 17(22): 2127-30, 1996.

126. **Zantop, T.; Weimann, A.; Schmidtko, R.; Herbort, M.; Raschke, M. J.; and Petersen, W.:** Graft laceration and pullout strength of soft-tissue anterior cruciate ligament reconstruction: in vitro study comparing titanium, poly-d,l-lactide, and poly-d,l-lactide-tricalcium phosphate screws. *Arthroscopy,* 22(11): 1204-10, 2006.

127. **Zhang, E.; Xu, L.; Yu, G.; Pan, F.; and Yang, K.:** In vivo evaluation of biodegradable magnesium alloy bone implant in the first 6 months implantation. *J Biomed Mater Res A*, 2008.

CURRICULUM VITAE

1 PERSÖNLICHE DATEN

Name:	Richard Lindtner
Geburtsdaten:	06.07.1982, Hallein
Staatsbürgerschaft:	Österreich
Familienstand:	ledig
Adresse:	Griesstraße 4
	5450 Werfen
Telefon:	(0650) 58 08 250
Email:	r.lindtner@gmx.at

2 SCHULBILDUNG

09/1988-07/1992	Volksschule Werfen
09/1992-07/2000	Missionsprivatgymnasium St. Rupert, Bischofshofen

10/2000-10/2001	Zivildienst als Rettungssanitäter beim Österreichischen Roten Kreuz

3 AKADEMISCHE AUSBILDUNG

10/2001-07/2002	Universität Salzburg: Philosophie, Latein und Germanistik
seit 10/2002	Medizinische Universität Graz

1. Abschnitt: 10/2002-07/2003
2. Abschnitt: 10/2003-07/2008
3. Abschnitt: 10/2008-07/2009

4 ZUSATZQUALIFIKATIONEN, SCHWERPUNKTE UND FREIWILLIGE AUSBILDUNG

ZUSATZQUALIFIKATIONEN

- Studienassistent am Anatomischen Institut der Medizinischen Universität Graz (10/2007 – 12/2008)
- Rettungssanitäter beim ÖRK (seit 01/2001)

SCHWERPUNKTSETZUNG WÄHREND DES STUDIUMS

- SSM `Von der Theorie zur Praxis: Chirurgische Operationslehre´
- SSM `Klinisch-topographische Anatomie der Extremitäten´
- SSM `Klinisch-topographische Anatomie der Eingeweide´
- SSM `Klinisch-topographische Anatomie des Kopfes und Halses´

FREIWILLIG ABSOLVIERTE AUSBILDUNGEN

- Spezielles Schockraum-Management Schwer- und Mehrfachverletzter (Prof. Szyskowitz)
- AO-Workshop „Fracture Treatment Growth“ (Kursleiterin: PD A.M. Weinberg, 15.September 2007, Graz)
- Common invasive procedures I
- Common invasive procedures II
- Phantomübungen für Anästhesiologie und Notfallmedizin (Prof. Schwarz)
- Prognosefaktoren in der Tumorpathologie (LV für Dissertanten) (Doz. Langner)

5 FAMULATUREN

12.09.-30.09.2005 Unfallchirurgie und Sporttraumatologie,
Kardinal Schwarzenberg´sches Krankenhaus, Schwarzach

06.02.-18.02.2006 Visceral- und Thoraxchirurgie,
Universitätsklinikum Salzburg

10.07.-11.08.2006 Unfallchirurgie und Sporttraumatologie,
Universitätsklinikum Innsbruck

21.08.-01.09.2006 Herzchirurgie,
Universitätsklinikum Salzburg

09.07.-03.08.2007 Innere Medizin und Notfallmedizin (NEF-Einsätze)
Kardinal Schwarzenberg´sches Krankenhaus, Schwarzach

6 KLINISCH-PRAKTISCHES JAHR

01.10.-11.12.2008 Innere Medizin,
Krankenhaus der Barmherzigen Brüder Marschallgasse, Graz

12.12.08-30.01.09 Kinderkardiologie,
Universitätsklinikum Graz

02.03.-03.04.2009 Allgemeinmedizin,
Dr. Viktor Schwab, Abtenau

20.04.-03.07.2009 Unfallchirurgie,
Universitätsklinikum Graz

7 WISSENSCHAFTLICHE TÄTIGKEIT

PATHOLOGIE

Seit Jänner 2005 Mitarbeit am Aufbau eines Forschungsschwerpunktes zu Colorectalen Carcinomen am Institut für Pathologie der Medizinischen Universität Graz unter der Leitung von Univ.-Doz. Dr. Cord Langner.

UNFALLCHIRURGIE

Seit Juli 2007 Mitarbeit an mehreren Projekten in der traumatologischen Forschungsgruppe um Privatdozentin Annelie Maria Weinberg, Leiterin der Wissenschaftlichen Abteilung für Unfallforschung und -prophylaxe an der Universitätsklinik für Kinderchirurgie in Graz.

8 PUBLIKATIONS- UND VORTRAGSLISTE

CASE REPORTS UND LETTERS TO THE EDITOR

Lindtner RA, Schreiber F, Langner C.: Cytokeratin 7 immunostaining facilitates recognition of pancreatic heterotopia in gastric biopsies.
Pathol Int. 2007 Aug;57(8):548-50.

Lindtner RA, Ott A, Schweiger W, Langner C.: Synchronous multifocal colorectal and kidney cancer in a patient with longstanding history of ulcerative colitis.
Inflamm Bowel Dis. 2007 Apr 6;13(9):1186-1188

ABSTRACTS VON KONGRESSBEITRÄGEN (VORTRÄGE [VO] & POSTER [P]))

Lindtner RA, Kornprat P, Pollheimer VS, Pollheimer MJ, Rehak P, Langner C: Is the Prognostic Significance of Lymphatic and Venous Invasion in Colorectal Cancer Related to Vessel Location?
Österreichische Gesellschaft für Chirurgie, 49. Österreichischer Chirurgenkongress, May 21-23, Innsbruck, Austria
European Surgery, 40 (Supplement 224): 52- 53, 2008 [VO]

Lindtner RA, Langner C, Pollheimer MJ, Pollheimer VS, Rehak P, Kornprat P: Does pT2 and pT3 Subclassification in Colorectal Cancer Facilitate Outcome Prediction in Affected Patients?
Österreichische Gesellschaft für Chirurgie, 49. Österreichischer Chirurgenkongress, May 21-23, Innsbruck, Austria
European Surgery, 40 (Supplement 224): 95, 2008 [P]

Kornprat P, **Lindtner RA**, Pollheimer VS, Pollheimer MJ, Mischinger H, Langner C: Impact of Tumour Size on Patients Outcome in Colorectal Cancer.
Österreichische Gesellschaft für Chirurgie, 49. Österreichischer Chirurgenkongress, May 21-23, Innsbruck, Austria
European Surgery, 40 (Supplement 224): 95, 2008 [P]

Langner C, **Lindtner RA**, Pollheimer MJ, Pollheimer VS, Kornprat P, Schlemmer A, Rehak P, Kapp K, Berger A, Hoefler G: Colorectal Cancer in Styria / Southern Austria (CCS-Project): Changing Patterns over a Period of 20 Years.
European Multidisciplinary Colorectal Cancer Congress, Feb 24-26, Berlin, Germany
Ann Oncol, 19 (Supplement 1): 134, 2008 [P]

Pollheimer MJ, Pollheimer VS, **Lindtner RA**, Schlemmer A, Langner C: Syn- and/or Metachronous Occurrence Colorectal and Renal Cell Carcinoma: No Evidence for a Clinical Entity.
European Multidisciplinary Colorectal Cancer Congress, Feb 24-26, Berlin, Germany
Ann Oncol, 19 (Supplement 1): 135, 2008 [P]

Pollheimer VS, Pollheimer MJ, **Lindtner RA**, Hoefler G, Schlemmer A, Langner C: Is the Syn- and/or Metachronous Occurrence of Colorectal Carcinoma and Urothelial Carcinoma of the Upper Urinary Tract related to Lynch Syndrome?
European Multidisciplinary Colorectal Cancer Congress, Feb 24-26, Berlin, Germany
Ann Oncol, 19 (Supplement 1): 135, 2008 [P]

Fischerauer EE, Janezic G, Gülly C, Amerstorfer F, Gaber S, Blümel P, Castellani C, Hausbrandt P, **Lindtner RA**, Weinberg AM: Molecular insights into growth plate phenomenons due to diaphyseal fracture - molecular and functional analyses.
ZMF DAY Medical University of Graz, November 21, Graz, Austria
Abstractbook: 93, 2007 [P]

Lindtner RA, Pollheimer MJ, Pollheimer VS, Wegscheider BJ, Schlemmer A, Langner C: Changes in Colorectal Cancer Presentation during a 20-Year Period: A Large Single Centre Experience.
Adriatic Society of Pathology, 21st International Meeting, Jun 24-25, Trieste, Italy
Abstractbook: Abstract No. 5, 2006 [VO]

Pollheimer VS, Winkler A, Pollheimer MJ, **Lindtner RA**, Hoefler G, Schlemmer A, Langner C: Is the Syn- and/or Metachronous Occurrence of Colorectal Carcinoma and Urothelial Carcinoma of the Upper Urinary Tract related to HNPCC?
Adriatic Society of Pathology, 21st International Meeting, Jun 24-25, Trieste, Italy
Abstractbook: Abstract No. 2, 2006 [VO]

Pollheimer MJ, Pollheimer VS, **Lindtner RA**, Schlemmer A, Langner C: Syn- and/or Metachronous Occurrence of Colorectal and Renal Cell Carcinoma: No Evidence for a Clinical Entity
Adriatic Society of Pathology, 21st International Meeting, Jun 24-25, Trieste, Italy
Abstractbook: Abstract No. 7, 2006 [VO]

WEITERE VORTRÄGE (nicht zitierfähig)

Castellani C, Hausbrandt P, **Lindtner RA**, Fischerauer E, Weinberg AM: New Biodegradable Implants in Growing Rats.
Internal presentation, Synthes, Apr, Oberdorf, Switzerland, 2008 [VO]

Castellani C**,** Hausbrandt P, **Lindtner RA**, Fischerauer E, Weinberg AM: Inflammatory reaction and biocompatibility of new biodegradable implants in growing rats.
Internal presentation, ZMF, Medizinische Universität Graz, Feb 13, Graz, Austria, 2008 [VO]

Fischerauer EE, Janezic G, Amerstorfer F, Gaber S, Bluemel P, Castellani C, **Lindtner RA**, Hausbrandt P, Seles M, Gross S, Weinberg AM: Growth disturbances due to diaphyseal fracture/growth plate lesions during growth.

Klausurtagung der Deutschen Akademie der osteologischen und rheumatologischen Wissenschaften, Feb 16, Graz, Austria, 2008 [VO]

Lindtner RA: K-wire osteosynthesis - Technique and indications.AO-Workshop „Fracture Treatment Growth“, Sept 15, Graz, Austria, 2007 [VO]